Influence of Acidity and Alkalinity of Water Environments on the Water Stability of Asphalt Mixture: Phase I - Molecular Dynamics Simulation

Derun Zhang[a]; Pei Yu[a]; Ziyang Liu[a]; Zhiyang Liu[b]; Hui Chen[c]; Yangming Gao[d*]

[a] *School of Civil and Hydraulic Engineering, Huazhong University of Science and Technology, Wuhan 430074, China*

[b] *College of Civil and Transportation Engineering, Shenzhen University, Shenzhen 518061, China*

[c] *Texas A&M Transportation Institute, Texas A&M University, College Station, Texas 77807, United State*

[d] *School of Civil Engineering and Built Environment, Liverpool John Moores University, Liverpool, United Kingdom*

* *Corresponding Authors:* y.gao@ljmu.ac.uk

Abstract

The pH of the water environment of asphalt pavement is not constant at 7.0. Existing studies have shown that the erosion of asphalt mixtures may be more severe in acidic or alkaline water environment. However, the mechanism of water damage of asphalt mixture in acidic or alkaline water environment has not yet been clear so far. To fulfill this research gap, the molecular dynamics (MD) simulation was employed in this study to explore the erosion mechanism of acidic and alkaline aqueous solutions on asphalt and asphalt-aggregate interface. The 12-component AAA-1 asphalt model was used to represent asphalt, while the calcite and quartz were selected to represent the limestone and granite, respectively. Asphalt-solution system and asphalt-aggregate interface system under different water environments were established. Through investigating the nanostructure change of the asphalt-aggregate system, the relative concentration (RC) and mean square displacement (MSD) of asphalt molecules, and the adhesion between asphalt and aggregate were analyzed. The mechanism pertaining to the performance degradation of asphalt and asphalt-aggregate systems under different water environments was unveiled. The results show that the nanostructure of asphalt may change under the acidic and alkaline water environments, which may further lower the cohesion of asphalt. In addition, the acidic and alkaline aqueous solutions will change the molecular structure of asphalt-aggregate interface by promoting the molecular migration of four asphalt components, including the saturates (S), aromatics (A), resins (R) and asphaltene (A) components (SARA components), further affecting the water stability of asphalt mixture. These results are anticipated to provide new insights into the influence of acidic and alkaline water environments on the water stability of asphalt mixture from the molecular scale perspective.

Keywords: Asphalt mixture; Water environment; Water stability; Erosion mechanism; Molecular dynamic simulation.

1. Introduction

Water damage is one of the major forms of early damage of asphalt pavement. Its macroscopic manifestation is the detachment of asphalt binder from aggregate due to the action of water [1], which may lead to pothole, raveling or even the overall structural failure of asphalt pavement and therefore shorten the pavement service life. In essence, the water damage is mainly resulted from the cohesive failure of asphalt and/or the adhesive failure of asphalt-aggregate when water penetrates the asphalt film and arrives at the interface of asphalt-aggregate under the repeated vehicle loadings, as shown in Fig. 1 [2][3]. Thus, maintaining sufficient cohesion of asphalt and adhesion of asphalt-aggregate in presence of water plays an important role in the water stability of asphalt mixture [4][5].

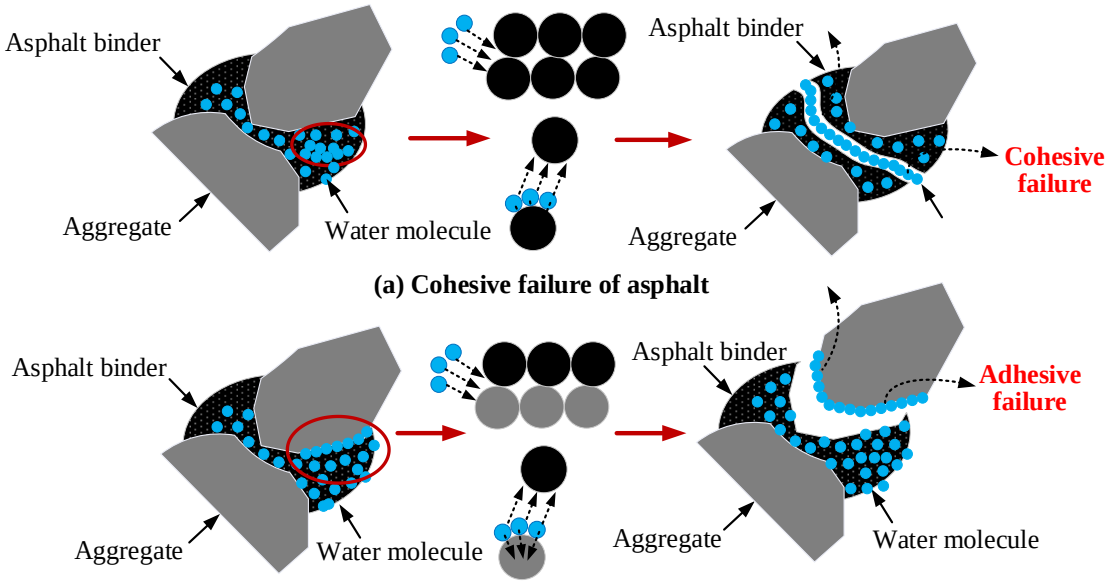

(a) Cohesive failure of asphalt

(b) Adhesive failure of asphalt-aggregate

Figure 1. Two failure types of water damage of asphalt mixture

Over the past few decades, considerable efforts have been devoted to evaluating the effect of water on the water stability of asphalt mixture from multi-scale perspectives. For instance, Moraes et al. used the bitumen bond strength (BBS) test to quantify the effect of moisture on the adhesion of asphalt-aggregate and verified the repeatability and reproducibility of the BBS test through statistical analysis [6]. Zhang et al. developed a pull-off test to determine the bonding strength of asphalt-aggregate under both dry condition and different water immersion conditions [7]. Liu and Xu et al. analyzed the micromorphological and chemical element changes of the aggregate-asphalt interface after water erosion using atomic force microscopy (AFM), scanning electron microscopy (SEM), and Fourier infrared transform spectroscopy (FTIR) [8][9]. To gain a better insight into the influence mechanism of water on the water susceptibility of asphalt mixture, the

molecular dynamics (MD) simulation has been widely used to simulate the interfacial interaction of asphalt-aggregate with and without the presence of water at a nano-scale (or molecular scale). For instance, Wang et al. predicted the adhesion strength of the quartz-asphalt interface at the nanoscopic scale for the first time through the simulated drawing tests. The simulation results showed that the interfacial stress-separation curve obtained from the MD simulation was consistent with the failure behavior measured from the macroscopic experiments [10]. Cui and Gao et al. used the MD simulation to study the adhesion of asphalt-aggregate and the distribution of asphalt components at asphalt-aggregate interface for different asphalt mixtures under the action of water [11]-[13]. Sun et al. evaluated the effect of asphalt aging on the water stability of asphalt mixture as well as the effect of four components of asphalt binder on the asphalt-aggregate adhesion through the MD simulation [14]. These studies indicate that the MD simulation method can effectively characterize the interfacial interaction between asphalt and aggregate at the nano-scale. However, at present the water environment in most of the MD simulation is neutral, which might not be able to fully capture the water environment of in-service asphalt pavement. In fact, the pH of the pavement water environment is not always constant at 7.0. Under the influence of acid and alkali rainfall, asphalt admixtures, pavement dust, and water-aggregate reaction, the pH of water environment may be altered. For instance, Arabani et al. [15] collected the surface water from some road pavements that had different traffic volumes and found that surface dust and soot generated by automobiles can change the pH value of the road surface water, which fluctuated between 6.16 and 8.06. Xie et al. [16] monitored the pH and iron types of rainfall for 291 cities in China from 2003 to 2018. The collected data indicated that the pH of the rainfall changed in a wide range, and the anions in acid rain were identified to mainly consist of sulfate ions (SO_4^{2-}) while the cations in alkali rain mainly ammonium ions (NH_4^+). Yoon and Tarrer [17] added several different types of aggregate powders into natural water and found that the pH of the water gradually increased to a relatively high value. This phenomenon can be ascribed to the reaction between the water and the aggregate powders. Indicatively, most of the aggregate powders contain mental ions such as Na^+, K^+, and Ca^{2+}. These mental ions can be exchanged with protons when the aggregate powders come into contact with water, leading to the hydroxyl ions produced to increase the pH of the surrounding aqueous phase by several units.

The alteration of water pH may further affect the water stability of asphalt pavement. For instance, Hu et al. evaluated the water stability of semi-flexible pavement under the corrosion of different types of acid rain ($pH < 7.0$) through the immersion Marshall test, freeze-thaw splitting test and vacuum saturation test. It was found that the acidification of rainwater can decrease the ductility, viscosity and plasticity of asphalt, which further weakened the binding force between the asphalt and limestone aggregate and led to the decline of

water stability of asphalt pavement [18]. Yoon and Tarrer [17] conducted a series of boiling water tests to assess the sensitivity of asphalt stripping from the aggregate to the changes in the water pH, which was achieved by modifying the water with addition of HCl or NaOH solution. They observed that the stripping became more severe when the pH value increased from 2.0 to 7.0 for the granite aggregate, and from 3.0 to 13.0 for the chert gravel, implying that different types of aggregate had different stripping potentials with respect to the same pH water environment. Hughes et al. [19] measured the interfacial tensions and contact angles between asphalt-aggregate suspended in buffered solutions at five different pH values (pH = 6.0, 7.0, 8.0, 8.5, and 9.0) through capillary rise method and sessile drop method, respectively. Then the adhesion tension values of asphalt-aggregate were calculated from the measurements. The calculation results showed a general trend that the adhesion tension decreased as the pH of the buffered solution increased, and the adhesion tension became even negative at alkaline water environment, namely pH = 8.5 and pH = 9.0.

Previous studies state clearly that the change in the pH of the water environment may have a significant impact on the water stability of asphalt mixture. However, most of the studies focused mainly on assessing the influence of water pH on the overall performance degradation of asphalt mixture, which can be categorized as macroscopic examination. Very little attention has been paid so far on the degradation mechanism of asphalt mixture performance resulted from the change of the water pH. To fulfill this research gap, the research team has conducted a systemic study to unveil the influence mechanism of the water pH on the water sensitivity of asphalt mixture at multiple scales, including the nano-scale, micro-scale and macro-scale. As phase I of the series of studies, this paper was aimed to investigate the influence of water pH on the water stability of asphalt mixture at nano-scale through the MD simulation.

2. Simulation models and methods

2.1 Molecular models

Asphalt binder is one of the main by-products of petrochemical. Its chemical composition is very complex and varies depending on the source of crude oil. Therefore, it is almost impossible to characterize the chemical composition of the asphalt binder using exact formulas **Error! Reference source not found.**. To address this issue, currently the most widely used method is to divide the asphalt binder into four major components, including the saturates (S), aromatics (A), resins (R) and asphaltene (A) components (SARA components) [12], and then combine these four components at varying proportions to establish the molecular dynamic models for characterize the properties of different types of asphalt binders. Such a SARA component model

was used firstly by the U.S. Strategic Highway Research Program (SHRP) to model eight asphalt binder, including AAA-1, AAK-1, AAM-1 and so on. Furthermore, Li and Greenfield et al. developed a 12-component AAA-1 asphalt binder model, in which the 12 components are representative of the SARA components of the asphalt binder [20]. A large number of studies have confirmed that this 12-component asphalt model has satisfactory accuracy for MD simulation [21]-[24], which will also be used in this study for the simulation purpose. The properties of these 12 components are listed in Table 1 and their molecular structures are given in Fig. 2.

Table 1 Composition of the 12-component model of AAA-1 asphalt binder

Label	Component	Compound	Molecular formula	Number of molecules	Mass fraction
As-1	Asphaltene	Asphaltene-phenol	$C_{42}H_{54}O$	6	17.14
As-2		Asphaltene-pyrrole	$C_{66}H_{81}N$	4	
As-3		Asphaltene-thiophene	$C_{51}H_{62}S$	6	
Re-1	Resin	Benzobisbenzothiophene	$C_{18}H_{10}S_2$	30	39.79
Re-2		Pyridinohopane	$C_{36}H_{57}N$	8	
Re-3		Quinolinohopane	$C_{40}H_{59}N$	8	
Re-4		Thioisorenieratane	$C_{40}H_{60}S$	8	
Re-5		Trimethylbenzeneoxane	$C_{29}H_{50}O$	10	
Ar-1	Aromatic	DOCHN	$C_{30}H_{46}$	26	31.94
Ar-2		PHPN	$C_{35}H_{44}$	22	
Sa-1	Saturate	Hopane	$C_{35}H_{62}$	8	11.13
Sa-2		Squalane	$C_{30}H_{62}$	8	

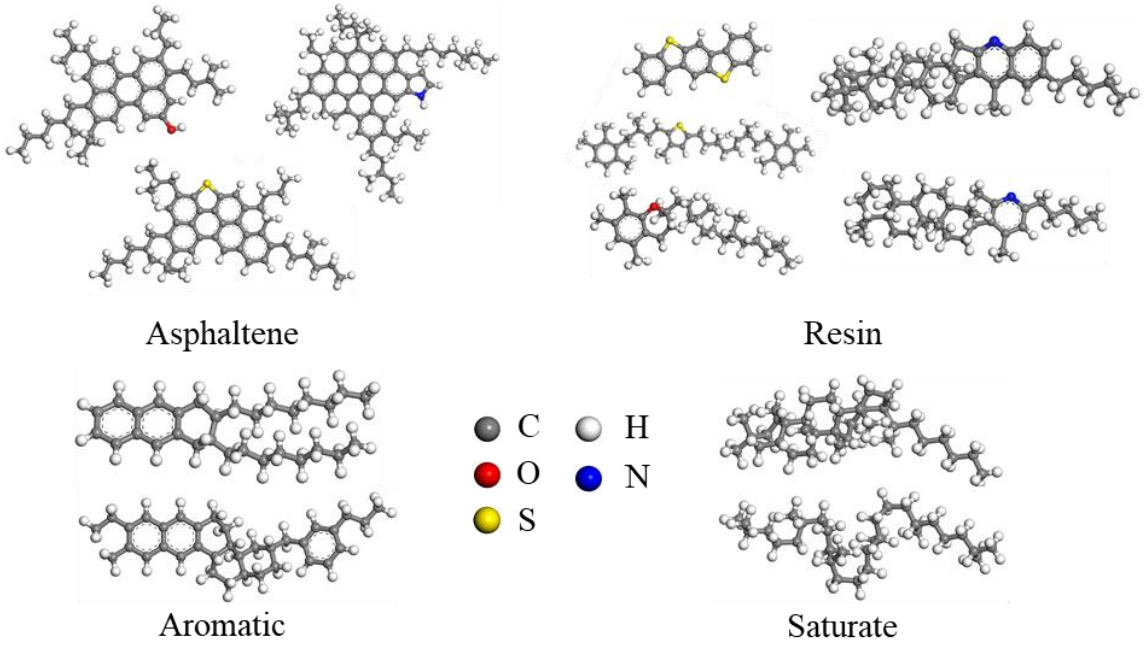

Fig. 2. Molecular structures of the 12 components of the AAA-1 asphalt binder

In order to verify the rationality of the simulation parameters, a cubic asphalt bulk model was first constructed using the amorphous cell module embedded in Materials Studio. The 12-component molecules of the AAA-1 asphalt model were filled into a 3D periodic cube box at an initial density of 0.7 g/cm^3. After running 2000 steps of the geometry optimization of the asphalt model, the MD simulation was carried out for 300ps at a step size of 1fs with isothermal-isobaric (NPT) ensemble (at 298K and 1 standard atmosphere) to reduce the box volume until the box size and system energy kept unchanged. Subsequent to this, a 100ps dynamics equilibration was performed with canonical ensemble (NVT) at 298K to reach a steady state. The asphalt density increased rapidly at the first 25ps and then gradually reached a steady state with a value of approximately 1.003 g/cm^3, as shown in Fig. 3. Compared with previous experimental and simulation results [14][20][26][27], the constructed model has a similar density, which therefore can be considered as a reliable asphalt model.

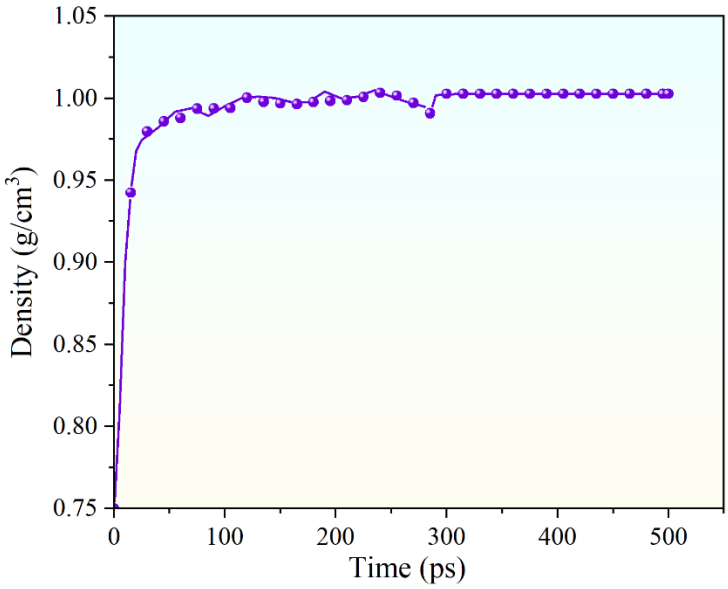

Fig. 3. Evolution of asphalt density with simulation time

After determining the asphalt density, the asphalt and asphalt-aggregate models in different water environments were established to explore the erosion mechanism of asphalt and asphalt mixture subjected to different acidic and alkaline water environments. Periodic cubic asphalt simulation systems were developed, which were composed of asphalt and water molecules at a mass ratio of 1:2, as exhibited in Fig. 4(a)-(c). In these systems, 50 sulfuric acid and 100 ammonia water molecules were added to the acidic and alkaline water environments, respectively. Based on the asphalt density obtained from the previous simulation, the asphalt molecular layer was built up for the construction of the asphalt-aggregate interface model, as shown in Fig.

4(d). Noted that the length and width dimensions of the asphalt molecular layer need to be consistent with the aggregate substrate. After the geometric optimization of the asphalt layer model, the simulation temperature was set to 298K and a 100ps MD simulation was performed with NVT ensemble for the model to reach an equilibrium state. It is worth mentioning that the constructed model is aperiodic in the z-direction and has a flat surface, which is suitable for the development of the asphalt-aggregate interface system.

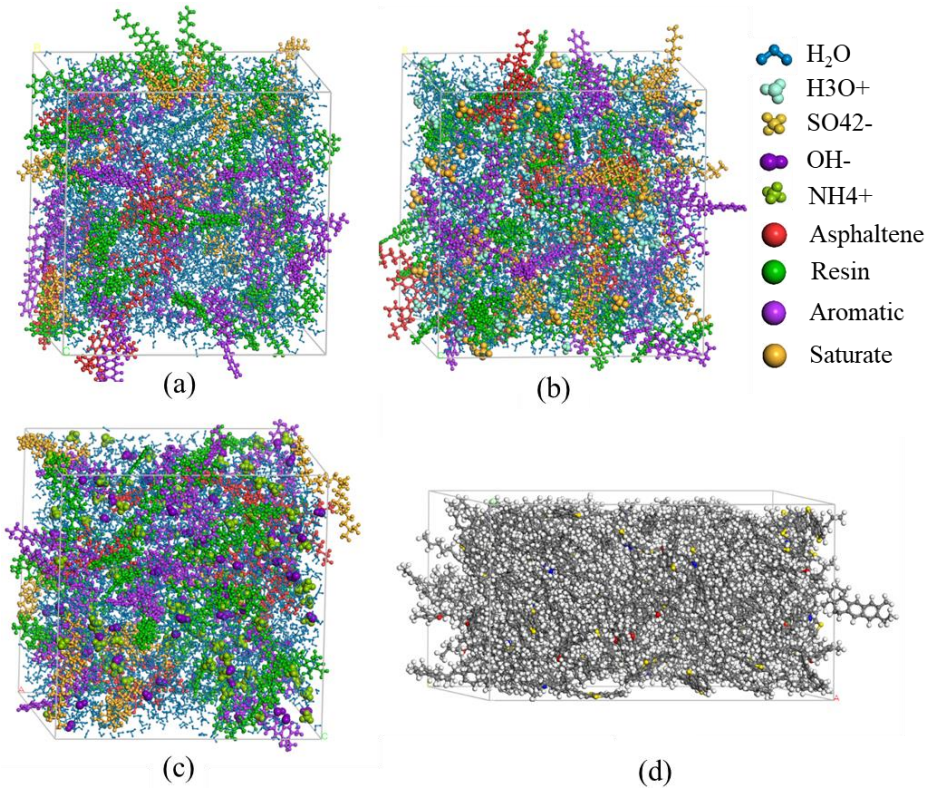

Fig. 4. Simulation systems of (a) asphalt-neutral water; (b) asphalt-sulfuric acid solution; (c) asphalt-ammonia solution; and (d) asphalt itself.

Quartz and calcite were used as aggregate substrates in this study, which represent acidic aggregate (granite) and alkaline aggregate (limestone), respectively. When constructing the aggregate model, quartz and calcite unit cells were first cleaved in the directions of (1 0 0) and (1 0 4) [13][28], respectively. Then the 2-D crystal surface was replicated in the x and y directions to construct the supercell planes. Next, a thin vacuum layer was added to the upper surface of this 2D structure to transform it into a 3D cuboid aggregate model with periodic boundary conditions imposed. The aggregates that were far away from the interface were fixed because they were hardly affected by the interfacial interaction. Noted that since silicon atoms on the surface of quartz have high hydrophilicity which are prone to hydration in the presence of water, aggregates having high silica content were simulated by adding two hydroxyl groups to each silicon atom on the surface [21][22]. Finally, after geometry optimization of the aggregate model, the simulated temperature was set to 298K and a

100ps MD simulation was performed with NVT ensemble so that the aggregate model can reach an equilibrium state. Fig. 5 presents the aggregate layer model used for the construction of the asphalt-aggregate interface system.

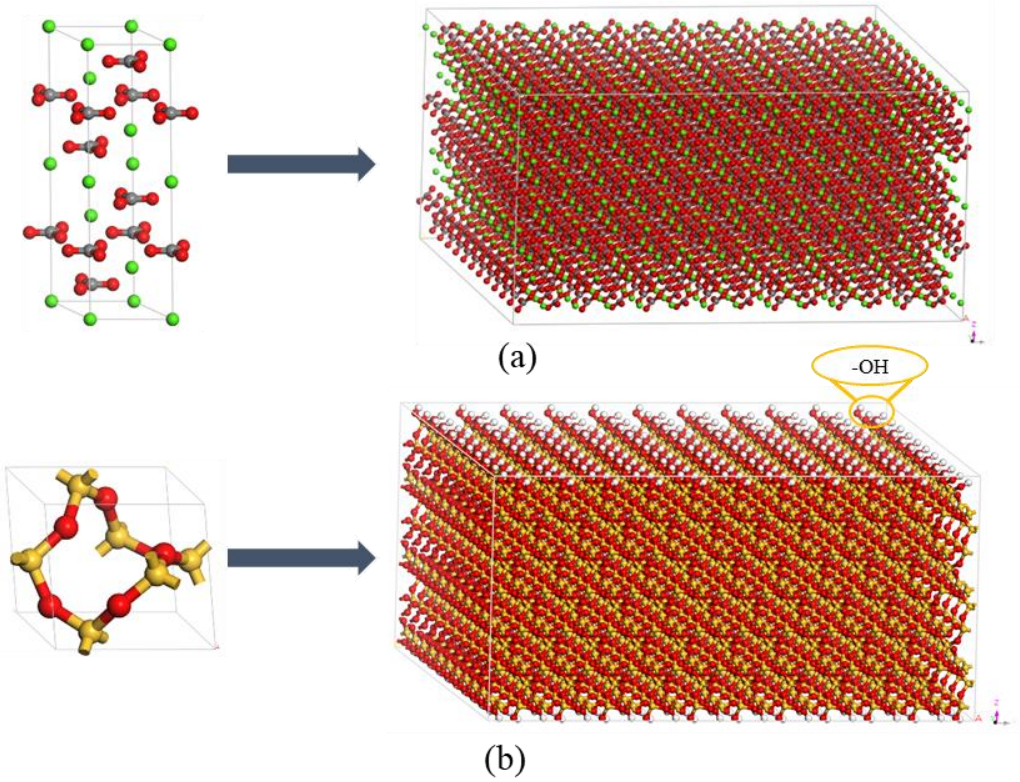

Fig. 5. Molecular models of crystal structure and layer of (a) calcite and (b) quartz aggregate.

After the asphalt layer model and the aggregate substrate models were built, the interface model can be constructed through attaching the asphalt layer shown in Fig. 4(d) to the surface of the aggregate layer. A vacuum layer with a thickness of 80 Å was added onto the upper surface of the asphalt layer to eliminate the influence of the 3D periodic boundary condition in the z direction. Based on this base model, the effect of different acidic and alkaline water environments on asphalt mixtures can be studied by incorporating an aqueous solution containing 200 water molecules to the asphalt-aggregate interface. As sated previously, the presence of water may facilitate the disruption of adhesion state of the aggregate-asphalt interface and therefore cause the asphalt film to detach from the aggregate surface, which is the root cause of water damage of the asphalt mixture. In this study, the sulfuric acid solution and ammonia aqueous solution were selected and used to represent the acid rainfall and alkaline rainfall, respectively. It should be emphasized that if the number of ions in acidic or alkaline solutions was determined according to the actual pH value of the water environment, it will lead to an extremely low content of solute ions or a very large number of water molecules in the simulation system. For example, the ratio of H^+ to H_2O in the solution is as low as 1:500 in terms of

iron or molecule number if pH = 1, which makes it very difficult to unveil the erosion mechanism of the acid ions on the asphalt-aggregate system. Therefore, in this study, the ratio of H^+ (or OH^-) to H_2O was set at 1:20, that is, the sulfuric acid solution contains 10 of H^+ ions and 5 of SO_4^{2-} ions, and the ammonia aqueous solution contains 10 of OH^- ions and 10 of NH_4^+ ions. Although this ratio is unable to reflect the pH value of the in-service pavement water environment, it could highlight the influence of sulfuric acid or ammonia water environment on the water stability of asphalt mixture. Fig. 6 exemplifies the simulation systems using calcite as aggregate in this study.

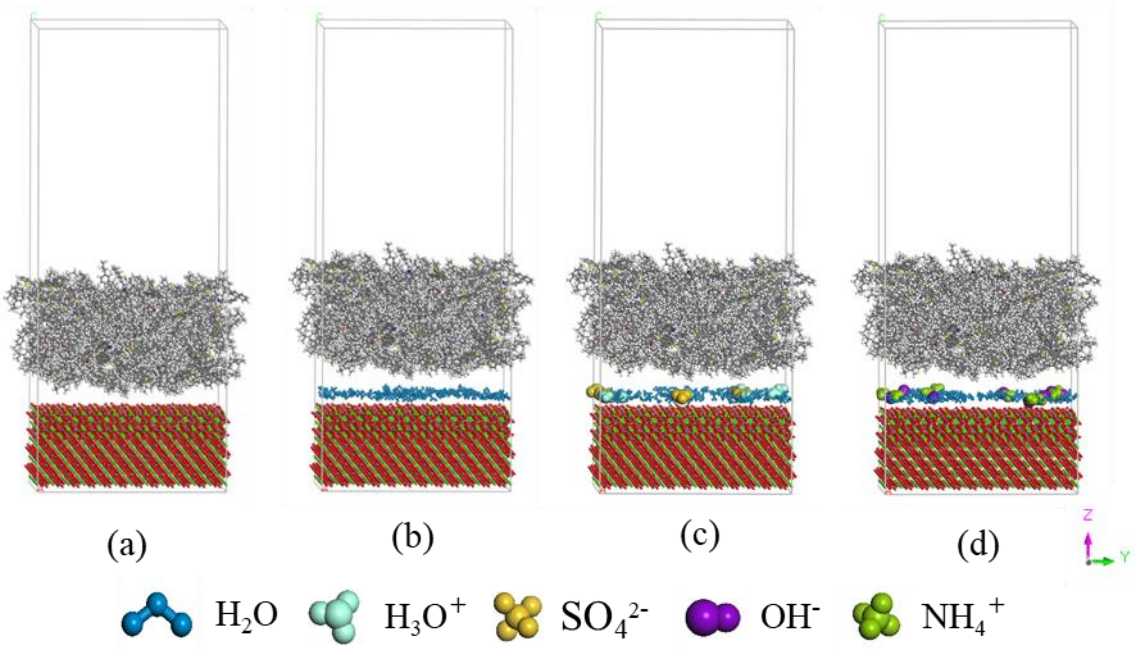

Fig. 6. Simulation systems of (a) calcite-asphalt; (b) calcite-neutral water-asphalt; (c) calcite-sulfuric acid solution-asphalt; and (d) calcite-ammonia solution-asphalt.

2.2 Simulation approach

In this study, the computer software Materials Studio was used to establish the molecular models for the characterization of thermodynamic properties of asphalt mixture. Before the MD simulation, it is necessary to determine the interatomic potential, which is the prerequisite for accurate determination of the interaction force between atoms. In this regard, an appropriate section of force field is very critical because it can accurately capture the nature of atomic interactions. To achieve this, the Condensed-phase Optimized Molecular Potentials for Atomistic Simulation Studies (COMPASS II) force field developed by Sun et al. was used to quantify the interatomic and intermolecular interactions in the system [29][30]. It is worthy to mention that this force field is the first ab initio forcefield that enables accurate and simultaneous prediction of

condensed-phase properties, including the equation of state, thermodynamical properties, molecular structure, interfacial failure mechanism and so on, for a diversity of molecular and polymers [31][32], which is also the first high quality forcefield to consolidate parameters of organic and inorganic materials. After the geometry optimization of 2000 steps, the molecular dynamics simulation was carried out with NVT ensemble at 298 K until an equilibrium state was achieved. As shown in Fig. 7, taking the interface model of asphalt-calcite under dry condition as an example, the temperature and energy of the system continuously changed with time and tended to be approximately constant after 20ps. After this critical point, variation of the amplitude of energy and temperature fluctuated within as low as 5%, the system can be therefore considered to reach equilibrium [33]. In order to further analyze the adhesion and molecular distribution of the simulation systems, another 300ps was assigned for the simulation run to achieve the equilibrium state under the same condition.

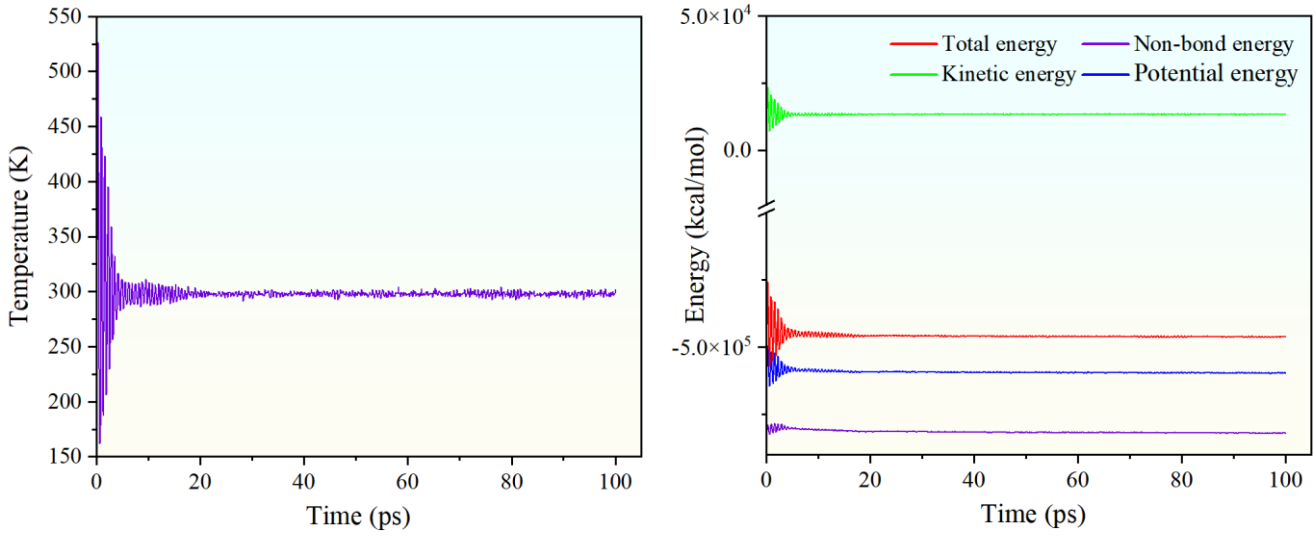

(a) **(b)**

Fig. 7. Evolution of (a) temperature and (b) energy of the simulation system within 100ps

2.3 Evaluation parameters

To evaluate the influence of acidity and alkalinity of water environments on the water stability of asphalt mixture from both qualitative and quantitative perspectives, the arrangement of molecules in the last frame trajectory of the simulation system was first obtained, and the effect of water environment on the nanostructure of asphalt and aggregate-asphalt system were then qualitatively analyzed. After that, the relative concentration (RC) analysis of the SARA components of asphalt in the last frame trajectory was carried out to obtain the distribution of these SARA components of asphalt under different conditions. The mechanism accounting for

the aggregate-asphalt adhesion change was explored based on the distribution of the SARA components of asphalt. Then, the mean square displacement (MSD) curve of the SARA components of asphalt on the aggregate surface was obtained from the trajectory of 5-295ps after the system reached equilibrium, and the molecular migration rate of asphalt on the aggregate surface under different acidic and alkaline water environments was calculated according to the slope of the MSD curve. Finally, the simulation data were extracted from the last frame of each simulation system to calculate the interaction, adhesion energy and debonding energy, which were then used for quantitatively evaluating the adhesion of asphalt components and aggregates and the water stability of aggregate-asphalt system under different acidic and alkaline water environments.

In order to analyze the distribution of the SARA components of asphalt on the aggregate surface, the relative concentration (RC) of each SARA component along the z direction in the interface model was calculated. To achieve this, the lattice was first divided into 100 bins along the direction of (0 0 1) to collect a sufficient amount of data [34]. Then the relative concentration was determined through the ratio of the mass concentration of certain type of molecule in each bin to the mass concentration in the entire lattice, as shown in Equations (1) and (2) [12][14]:

$$c_j = \frac{m_j}{v_j} \tag{1}$$

$$RC_j = \frac{c_j}{C_{total}} \tag{2}$$

where: c_j and C_{total} are the concentrations in the j^{th} bin and in the entire lattice, respectively; m_j is the atomic mass in the j^{th} bin; v_j is the volume of the j^{th} bin; RC_j is the relative concentration in the j^{th} bin.

The diffusion coefficient was used to characterize the mobility of asphalt molecules, which can be calculated through the Einstein equation, as given below [35][36]:

$$D = \lim_{t\to\infty} \frac{1}{6Nt} \sum_{i=1}^{N} \left| r_i(t) - r_i(0) \right|^2 \tag{3}$$

where: N is the number of atoms; t is the time interval; and $r_i(0)$ and $r_i(t)$ are the position vectors of the atomic center when it starts and ends within the time interval t.

Since MSD represents the average of the offsets of the positions of all particles in the system from their initial positions at any given time point, it is a function of time and can be calculated using Equation (4):

$$MSD = \frac{1}{N} \sum_{i=1}^{N} \left| r_i(t) - r_i(0) \right|^2 \tag{4}$$

Theoretically, after averaging all atomic mean square displacement, the MSD curve can be obtained as a function of time. In this sense, the diffusion coefficient D can be determined from the slope of the MSD curve based on Equation (5):

$$D = \frac{1}{6}\lim_{t\to\infty}\frac{d(MSD)}{dt} \tag{5}$$

From the above calculation equations, it can be seen that the MSD curve slope can be used to calculate the asphalt molecular migration capacity, and a larger value of the MSD curve slope is usually associated with a stronger capacity of the asphalt molecular migration. It is worth mentioning that for each asphalt component, its molecular migration properties may be related to its rheology.

For the sake of quantifying the adhesion between aggregate and asphalt, it is necessary to calculate the adhesion energy between aggregate and asphalt and between aggregate and individual asphalt component. In essence, adhesion energy is defined as the work required to separate the asphalt from the aggregate that is originally adhered to it, which reflects the bond strength at the asphalt-aggregate interface. Based on the MD results of the interface model constructed by the two aggregates in the environments of dry, neutral water, sulfuric acid solution and ammonia aqueous solution, the adhesion work and the adhesion energy can be calculated through Equations (6) and (7), respectively.

$$W_{adhesion} = \frac{\Delta E_{asp-agg}}{S} = \frac{E_{asp} + E_{agg} - E_{total}}{S} \tag{6}$$

$$E_{asp} = E_{\text{asphaltene}} + E_{resin} + E_{aromatic} + E_{saturate} \tag{7}$$

where: $\Delta E_{asp-agg}$ is the adhesion energy between asphalt and aggregate under the dry condition; E_{asp} and E_{agg} are the potential energy of asphalt and aggregate, respectively; E_{total} is the potential energy of aggregate-asphalt; $E_{asphaltene}$, E_{resin}, $E_{aromatic}$, and $E_{saturate}$ are the potential energy of asphaltene, resin, aromatic and saturate, respectively; and S is the interface area of aggregate-asphalt.

In the COMPASS II force field, the potential energy includes the bonded and non-bonded components, which can be represented using a summation:

$$E = E_{val} + E_{non} \tag{8}$$

where: E is the potential energy; E_{val} is the bonded potential energy component; and E_{non} is the non-bonded potential energy component, which is mainly composed of van der Waals force (E_{vdW}) and Coulomb force (E_Q) and can be calculated through the following equations.

$$E_{non} = E_{vdW} + E_Q \tag{9}$$

$$E_{vdW} = \sum_{ij}\varepsilon_{ij}\left[2\left(\frac{r_{ij}^0}{r_{ij}}\right)^9 - 3\left(\frac{r_{ij}^0}{r_{ij}}\right)^6\right] \tag{10}$$

$$E_Q = \sum_{ij} \frac{q_i q_j}{r_{ij}} \tag{11}$$

where: r_{ij} is the distance between atom i and atom j; $\mathbf{r_{ij}^o}$ and $\boldsymbol{\varepsilon_{ij}}$ are the LJ-9-6 parameters of the i-j atomic pair, and q_i and q_j represent the charges of atoms i and j, respectively.

When the aqueous solution molecules invade the aggregate-asphalt interface, the asphalt will exhibit a tendency to be peeled off from the aggregate surface. The work required to separate the asphalt from the aggregate surface in the presence of different acidic and alkaline aqueous solutions is defined as debonding energy, which can be calculated using Equation (12) [37][38]:

$$W_{debonding} = \frac{\Delta E_{agg\_w} + \Delta E_{asp\_w} + \Delta E_{r,asp\_agg} - \Delta E_{asp\_agg}}{S} \tag{12}$$

where: $W_{debonding}$ represents the debonding energy of asphalt and aggregate under the wet condition; ΔE_{agg_w} represents the adhesion energy of aggregate and water; ΔE_{asp_w} represents the adhesion energy between asphalt and water; ΔE_{asp_agg} represents the adhesion energy between asphalt and aggregate under dry condition; and $\Delta E_{r,asp\_agg}$ represents the adhesion energy between aggregate and asphalt under wet condition.

Referring to previous studies [12], the water stability of asphalt mixture can be quantified by calculating the ratio of adhesion energy under the dry condition to debonding energy under the wet condition, which is expressed as below:

$$ER = \left| \frac{W_{adhesion}}{W_{debonding}} \right| \tag{13}$$

In general, a higher adhesion energy between aggregate and asphalt indicates that the asphalt binder is more difficult to peel off from the aggregate surface. In the meanwhile, a smaller absolute value of debonding energy corresponds to the lower degree of the replacement of asphalt binder by the water on the aggregate surface. Therefore, the higher the ER value, the lower the water sensitivity of the asphalt mixture [12][39][40].

3. Results and discussion

3.1 Effect of acidity and alkalinity of aqueous solution on the behavior of asphalt molecules

After 300ps simulation, the distribution of molecules in the asphalt-solution two-phase system is shown in Fig.8. The red dash lines divide each of the sub-figures into four parts. Each part corresponds to an original simulation box, which was periodically displayed along the x and y axis to obtain the other three boxes. The aim was to show more clearly the nanostructure of the asphalt binder under the influence of different aqueous solutions. It is evident that after achieving equilibrium, water molecules and asphalt molecules are distributed

separately in different areas. Indicatively, water molecules are almost absent within the equilibrium asphalt structure. Also, resin and aromatic molecules interact directly with the aqueous solution at the asphalt-solution interface, but asphaltene molecules that possess strong polarity are mainly distributed in the interior of the asphalt structure. This phenomenon may be ascribed to the size effect of resins, aromas and asphaltenes. Among them, asphaltene molecules include 5~12 condensed aromatic rings with a relative molecular weight of approximately 500~900, while resin and aromatic molecules have only 2~6 fused rings and long aliphatic chains with a relative molecular weight of about 300~600. Resin and aromatic components with smaller molecules migrate to the surface and expose the fused rings to the water environment, while the hydrophobic long aliphatic chains move inward, impeding the migration of asphaltene molecules to the water environment.

Distinct difference in the nanostructure of asphalt can be observed in different aqueous solutions. For instance, in the neutral and acidic solution environments (Fig.8(a)(b)), the aqueous solution molecules are aggregated together inside, while the asphalt molecules are distributed around the solutions in a grid-like pattern. More specifically, the distribution area of the concentrated water molecules in the sulfuric acid solution (Fig.8(b)) is larger than that in the neutral water environment, while the asphalt molecules have a relatively smaller distribution area. This is plausible because the SO_4^{2-} ions in the sulfuric acid solution are capable to attract more water molecules so that water molecules gather together more tightly, resulting in a thinner line of grid-like asphalt membrane. Therefore, under the influence of sulfuric acid solution erosion, the asphalt binder may be more prone to damage. In addition, when the asphalt binder is exposed to ammonia aqueous solution environment (Fig.8(c)), the asphalt molecules are distributed in a columnar pattern independent and parallel to each other, while the ammonia aqueous solution is distributed around the asphalt molecules. It can be readily inferred from these phenomena that the erosion of ammonia aqueous solution disrupts the interaction of asphalt molecules and destroys the structural integrity of the asphalt binder, which may further lead to serious deterioration of asphalt cohesion and asphalt-aggregate adhesion and cause the water damage of the asphalt mixture.

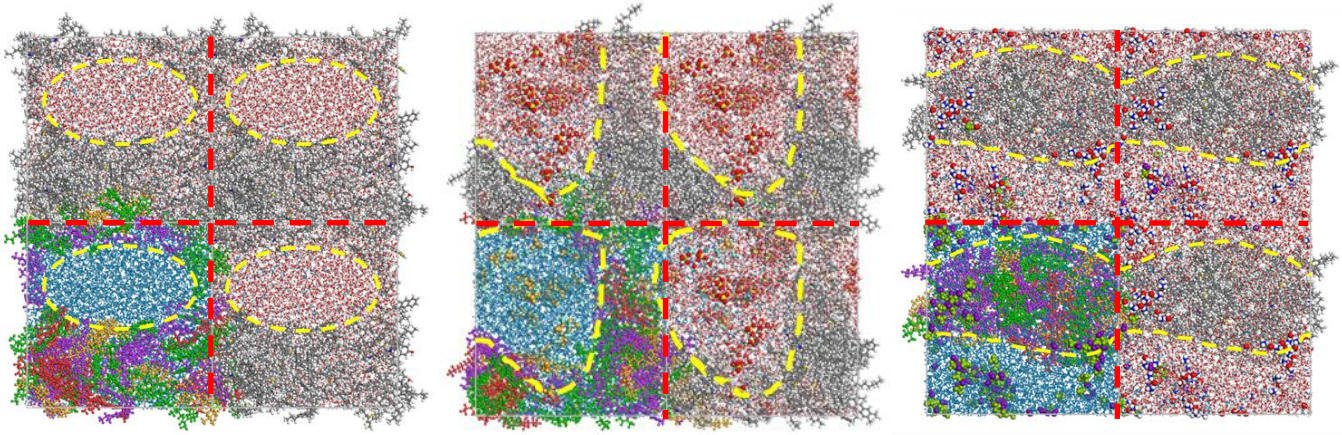

(a) **(b)** **(c)**

Fig. 8. Molecular configuration of asphalt-solution for the systems of (a) asphalt-neutral water; (b) asphalt-sulfuric acid solution; and (c) asphalt-ammonia alkaline solution.

3.2 Effect of acidity and alkalinity of aqueous solution on the interface characteristics of asphalt-aggregate

The molecular arrangement characteristics of the asphalt-calcite interface under four different environmental conditions are shown in Fig. 9. Apparently, in the dry environment (Fig. 9(a)), a gap between the calcite and asphalt molecules can be readily observed and the asphalt molecules are rearranged uniformly. As presented in Fig. 9(b)-(d), when the water molecules exist at the calcite-asphalt interface, they are evenly distributed on the aggregate surface due to their strong electrostatic interactions with the calcite aggregate. Indicatively, in the calcite-water-asphalt system, the oxygen atoms of the water and the anion sites on the benzene ring of asphaltene, resin and aromatic components will have a strong electrostatic interaction with the calcium ions of the calcite aggregate after an equilibrium is reached. In this regard, although the presence of water film facilitates the detachment of asphalt from the calcite aggregate surface, the polar components of the asphalt are still parallel to the water film, as exemplified in the enlarged view of molecular configuration of the asphalt-calcite in the neutral water environment, as shown in Fig. 10. The same parallel pattern of the molecular configuration of the asphalt-calcite can be also observed for the acid and alkaline water environments, as presented in Appendix Fig. 1-2. However, it should be noted that the distribution characteristics of the water molecules on the asphalt-calcite interface exhibit different patterns for the three different aqueous solutions, which can be directly reflected by the size of the gaps between the asphalt-water, as marked in Figure 9. Specifically, the asphalt-water has the largest size of gaps for the neutral water environment (Fig. 9(b)), followed by the sulfuric acid solution (Fig. 9(c)), and the ammonia alkaline solution has the smallest size of gaps (Fig. 9(d)).

The interaction energies of the calcite-water, asphalt-water, calcite-asphalt were extracted from the Materials Studio, which are summarized in Table 2. The interaction energy values of quartz-asphalt in the three different water environments are also included in this table, which will be used for the analysis of water stability of the quartz-asphalt system. Evidently, the absolute value of the interaction energy between ammonia aqueous solution and calcite is the largest, followed by that between sulfuric acid solution and calcite, and the absolute value of the interaction energy between neutral water and calcite is the smallest. It can be also observed from Table 2 that the same ranking applies to the interaction energy between the asphalt-aqueous solution. These stronger interactions between the solution-asphalt and between the solution-aggregate make the interaction between asphalt-aggregate weaker, which can be seen from the ranking of interaction energy of the asphalt-calcite system (absolute value) under the three different water environments, namely $\left|\Delta E_{asp\_agg\ (Neutral)}\right| > \left|\Delta E_{asp\_agg\ (H_2SO_4)}\right| > \left|\Delta E_{asp\_agg\ (NH_4OH)}\right|$. Thus, it can be concluded that the alternation of the

water pH weakens the adhesion between the asphalt-calcite and further reduces the water stability of the entire system.

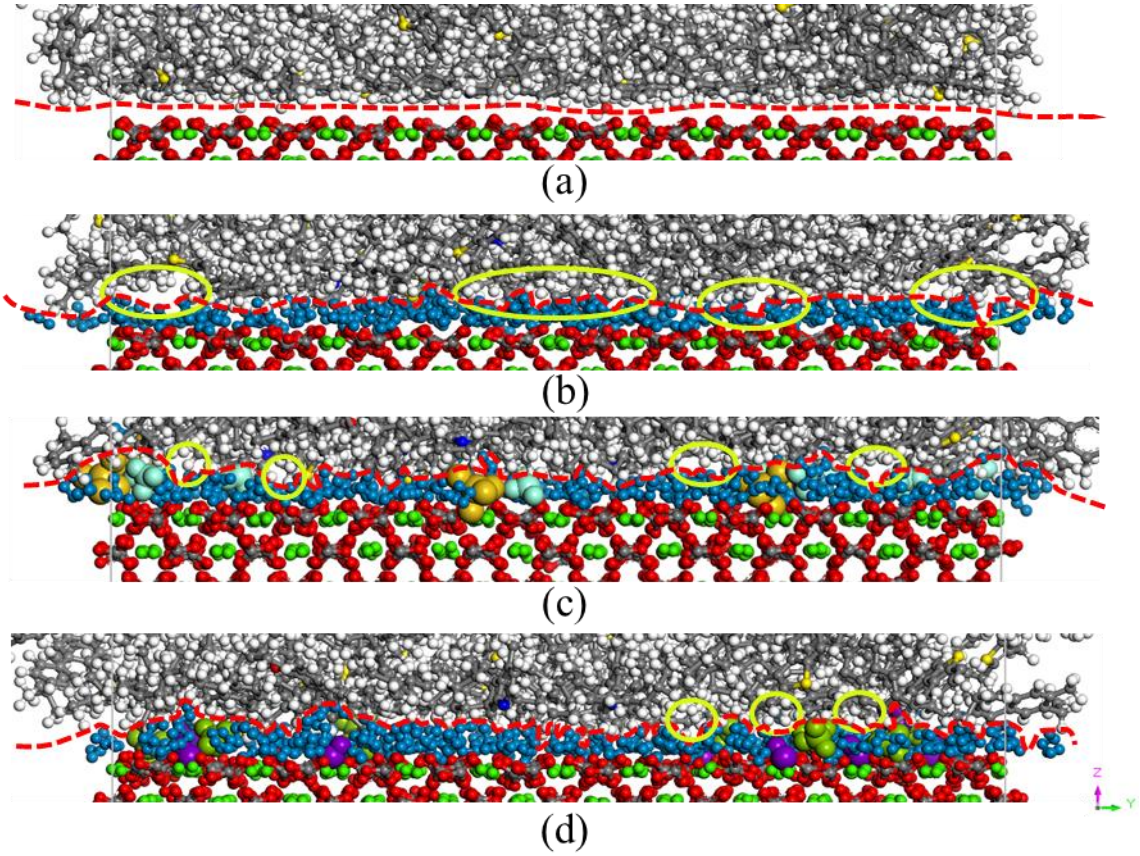

Fig. 9. Molecular structure of asphalt-calcite in (a) dry environment; (b) neutral water environment; (c) acidic water environment; and (d) alkaline water environment.

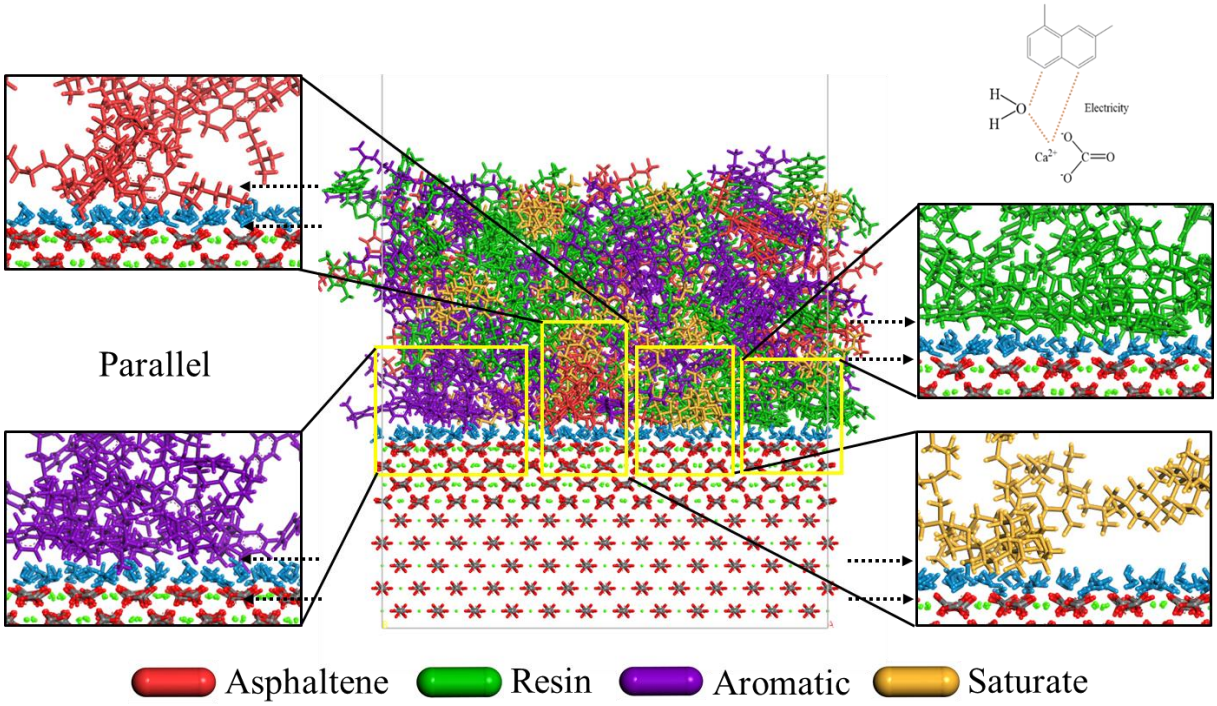

Fig. 10. Molecular interaction of asphalt-water-calcite system

Table 2 Interaction energy of asphalt-aggregate under different water environment conditions

Interaction energy	Calcite			Quartz		
	Neutral	H_2SO_4	NH_4OH	Neutral	H_2SO_4	NH_4OH
ΔE_{agg_w}	-4298.8	-4423.9	-5465.8	-510.9	-467.6	-446.9
ΔE_{asp_w}	-188.8	-203.4	-205.7	-185.5	-181.8	-218.0
ΔE_{asp_agg}	-381.0	-371.1	-357.1	-330.8	-355.0	-322.6

When looking into the asphalt-quartz system, as shown Fig. 11(a), in the dry environment, the asphalt molecules adsorbed on the silica surface are arranged in wave-like pattern. This is possibly due to that the van der Waals force between the quartz and asphalt molecules, which is usually manifested in a form of triangle. When water molecules invade the asphalt-quartz interface, the interaction between asphalt molecules and quartz extrudes on water molecules, making water molecules in the cone-shape. As shown in Fig. 11(b)-Fig. 11(d), water molecules, asphalt molecules, and quartz molecules coexist in a triangular structure at the interface for all the three water environments. Taking the neutral water environment for instance, as shown in Fig. 12, condensed aromatic rings and heteroatoms in the polar components of asphalt, oxygen atoms in water and hydroxyl groups on the surface of quartz are the active sites for intermolecular interactions. The same triangular pattern of the molecular configuration of the asphalt-quartz can be also seen for the acid and alkaline water environments, as presented in Appendix Fig. 3-4. These active sites have high electronegativity, which can produce the intermolecular interaction forces in the form of van der Waals forces. Besides, in the acidic and alkaline water environments, the interfacial molecular structure of asphalt-water-quartz system is different. In the acidic water environment, sulfate ions and hydrogen ions have strong electrostatic interaction with water molecules, driving more water molecules to be adsorbed on the aggregate surface. As a result, more asphalt molecules are in direct contact with the quartz aggregate in some specific surface regions, as shown in Figure 11(c). In the alkaline water environment, ammonium ions and hydroxide ions are relatively dispersed, leading to a wider distribution of water molecules on the quartz aggregate surface than that in neutral water environment, thereby increasing the stripping area between quartz aggregate and asphalt molecules. The increase in this stripping area severely weakens the van der Waals forces between the asphalt-aggregate, therefore imposing more water damage in the asphalt mixture. To gain a better visual comparison, the length of the asphalt-water-quartz system (in the direction of y axis) for the case that the water molecules have relatively low aggregation level is marked as L_b, L_c and L_d in Fig. 11(b)-Fig. 11(d), respectively. It can be easily inferred that a higher length value corresponds to a lower water susceptibility of the asphalt-aggregate.

In this sense, the water stability of the asphalt-quartz system for the different water environments has the following descending order: acidic water environment > neutral water environment > alkaline water environment. This finding is consistent with the interaction energy results presented in Table 2, where asphalt-quartz has the strongest interaction in sulfuric acid environment, followed by neutral water environment and the weakest interaction exists in ammonia water environment.

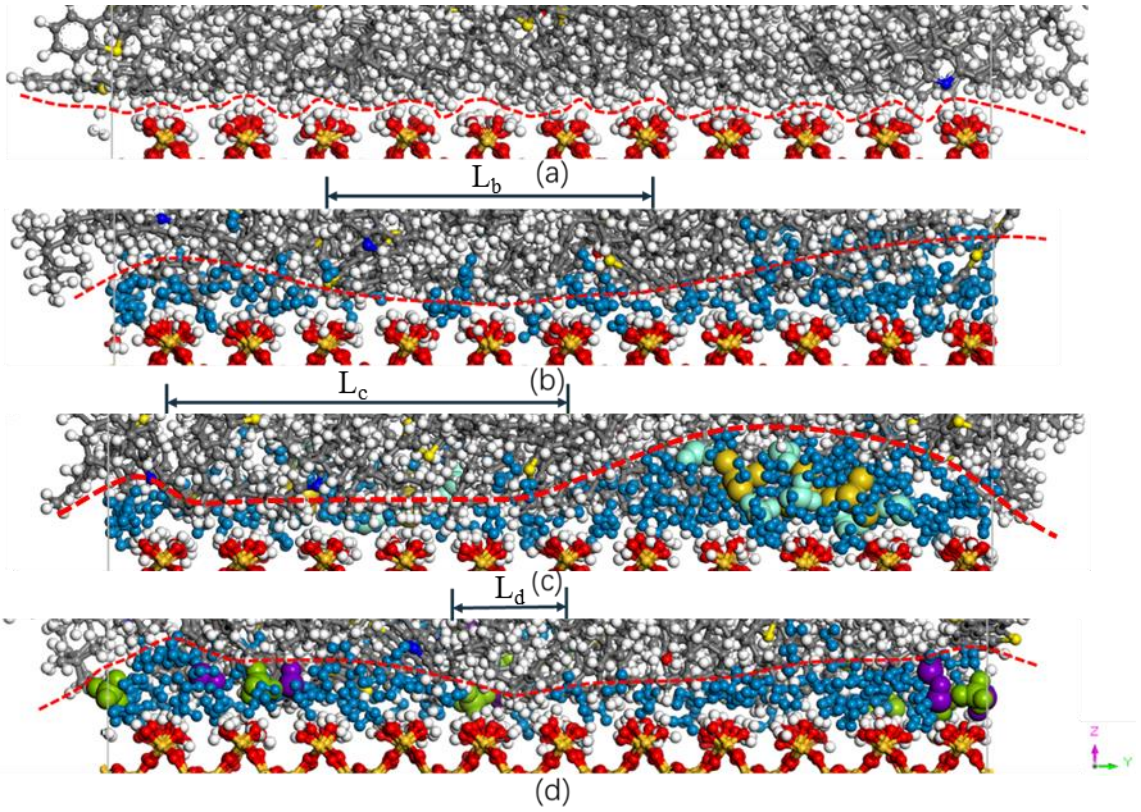

Fig. 11. Molecular structure of asphalt-quartz interface in (a) dry environment, (b) neutral water environment, (c) acidic water environment, and (d) alkaline water environment.

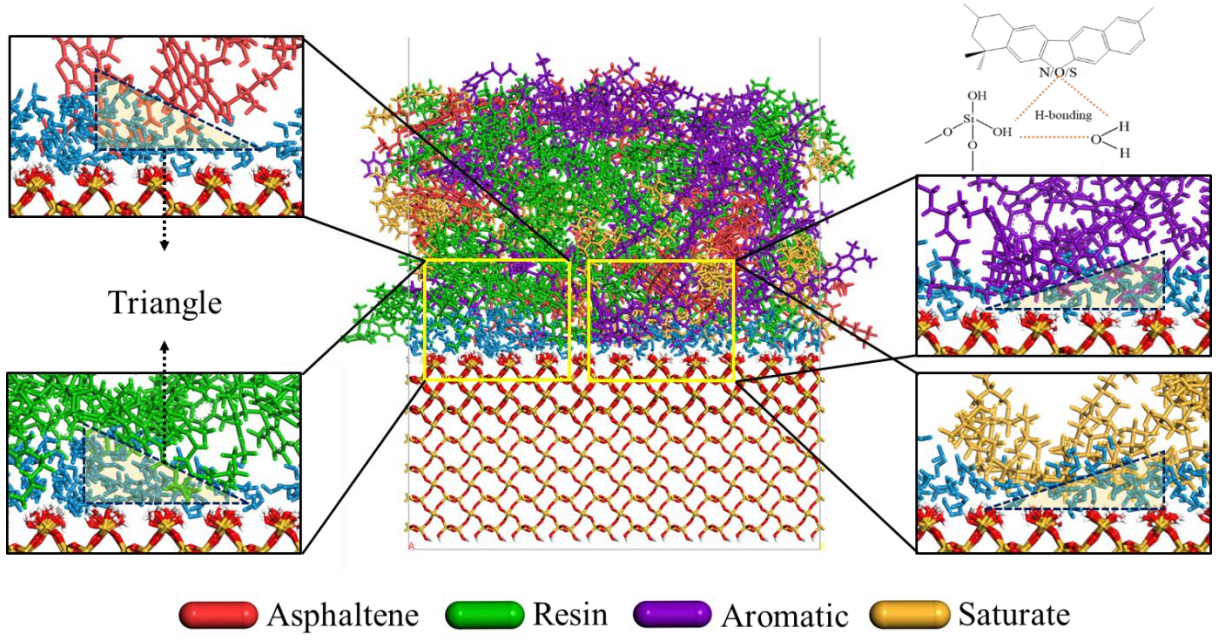

Fig. 12. Molecular interaction of asphalt-water-quartz system

3.3 Effect of acidity and alkalinity of aqueous solution on distribution characteristics of asphalt binder components

The intrusion of water can cause the concentration change of the four components of asphalt binder in the direction of z axis, as shown in Fig. 13. As is well known that when the water molecules exist at the asphalt -aggregate interface, the asphalt layer has a propensity of migrating away from the aggregate surface to increase the distance between asphalt and aggregate. Therefore, the relative concentration (RC) curves of the four components of asphalt move backwards as compared with those under dry condition. In addition, due to the different weight and polarity of the four components (SARA) of asphalt, the migration rates of these components are also different, which may further result in the change of the internal colloidal structure of the asphalt binder.

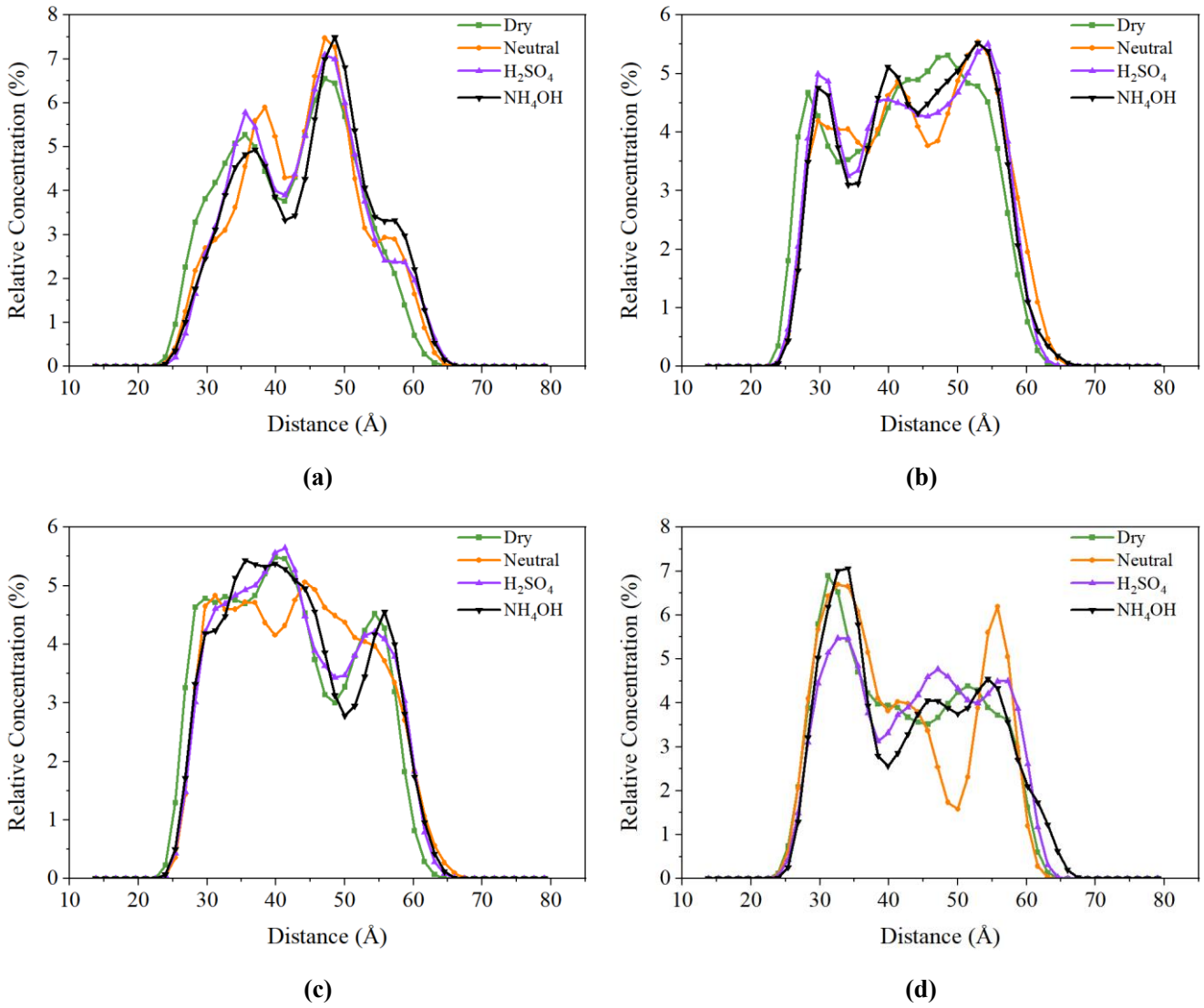

Fig. 13. Relative concentration distribution of SARA fractions in calcite-asphalt system under different environments along z direction: (a) Asphaltene, (b) Resin, (c) Aromatic, and (d) Saturate.

When calcite is used as aggregate, it can be seen from Fig. 13(a) that there is a significant difference in the distribution of asphaltene molecules under the three wet conditions. In the alkaline water environment, the RC curve of asphaltene molecule locates in a lower position than that of neutral water environment and acidic water environment in the range of 22Å-48Å from the bottom of the aggregate, while the RC curve is higher than that of the remaining two water environments in the range of 48Å-70Å from the bottom. However, in the acidic water environment, the RC value of asphaltene near the aggregate surface is higher than that in the neutral water environment. These findings indicate that compared with the neutral water, sulfuric acid solution will attract asphaltene molecules, while ammonia alkaline solution will repulse asphaltene molecules. The former will be beneficial for the water stability improvement and the latter will result in more severe water damage for the asphalt-aggregate system. From Fig. 13(b), it can be found that the first peak of the RC curve of resin under the dry condition appears near 28Å from the aggregate bottom, and the peaks move up to around 30Å under the three wet conditions. Among them, in the acidic and alkaline water environments, the peak value of RC curves of resin with respect to a small proportion of calcite aggregate surface is much greater than that in neutral water environment. These observations show that sulfuric acid and ammonia solutions produce stronger interaction with resin molecules. It is well recognized that resin molecules play a critical role in the adhesion between asphalt and aggregates[42]-[44]. However, the relative concentration of resin molecules is reduced when aqueous solution arrives at the interface, and the molecule location is far away from the aggregate. To this end, it can be concluded from these findings that the alternation of pH in the water environment have a potential to weaken the adhesion between asphalt and calcite aggregate. Additionally, as a weak polar and light component, the aromatic component also has a substantial influence on the asphalt-aggregate adhesion due to its large number of molecules. It can be seen from Fig. 13(c) that before 30 Å, the aromatic distribution pattern of the three wet environments is basically the same. In the range of 30Å-35Å, the relative concentration of aromatic in neutral water environment is slightly higher than that in acid and alkaline water environments. However, in the range of 35Å-45Å, the relative concentration of resin molecules in neutral water environment is much lower than that in the rest two water environments. This results in the lowest concentration of aromatic on the surface of calcite aggregate in neutral water environment. Saturate is a non-polar and lightweight component, which contributes less to the adhesion of asphalt aggregate as compared to the other three components. From 13(d), it can be seen that the saturation fraction under all the four conditions is mainly distributed near the surface of the aggregate, but its peak position lags behind the position where the resin and aromatic peaks appear. This may be due to the weaker electrostatic effect of the saturation component. When the resin and aromatic components migrate to the aggregate surface, the saturation component will be pushed away and move inwards the asphalt binder.

In the quartz-asphalt system, the four-component RC curves of asphalt on the aggregate surface in different environments are shown in Fig. 14. The RC curves of asphaltene in Fig. 14(a) exhibit different patterns in different wet environments. The peak value of the RC curve of asphaltene appears first in the

neutral water environment, and its value is roughly the same as that in the dry environment, but less than that in the acid water environment. In addition, the peak relative concentration of asphaltene in alkaline water environment is the lowest. In the range of 25Å-40Å, the concentration distribution of resin, aromatic and saturate is approximately identical. However, in the range of 40Å-50Å, the relative concentration of resin in neutral water environment shows a large peak, while that in acidic and alkaline water environments exhibits a downward trend. At the same time, the relative concentration of saturate fraction in alkaline water environment is much greater than that in neutral and acidic water environments. In contrast to the calcite system, the resin and aromatic components in the quartz system are distributed at a larger distance from the aggregate surface, while the saturate fraction is distributed closer to the aggregate surface. This may be due to the interaction between quartz and asphalt molecules in the form of van der Waals force, which decreases sharply when asphalt-quartz interface is invaded by the water molecules. However, they still have capability to make the saturate fraction with the lightest molecular weight migrate towards the aggregate surface.

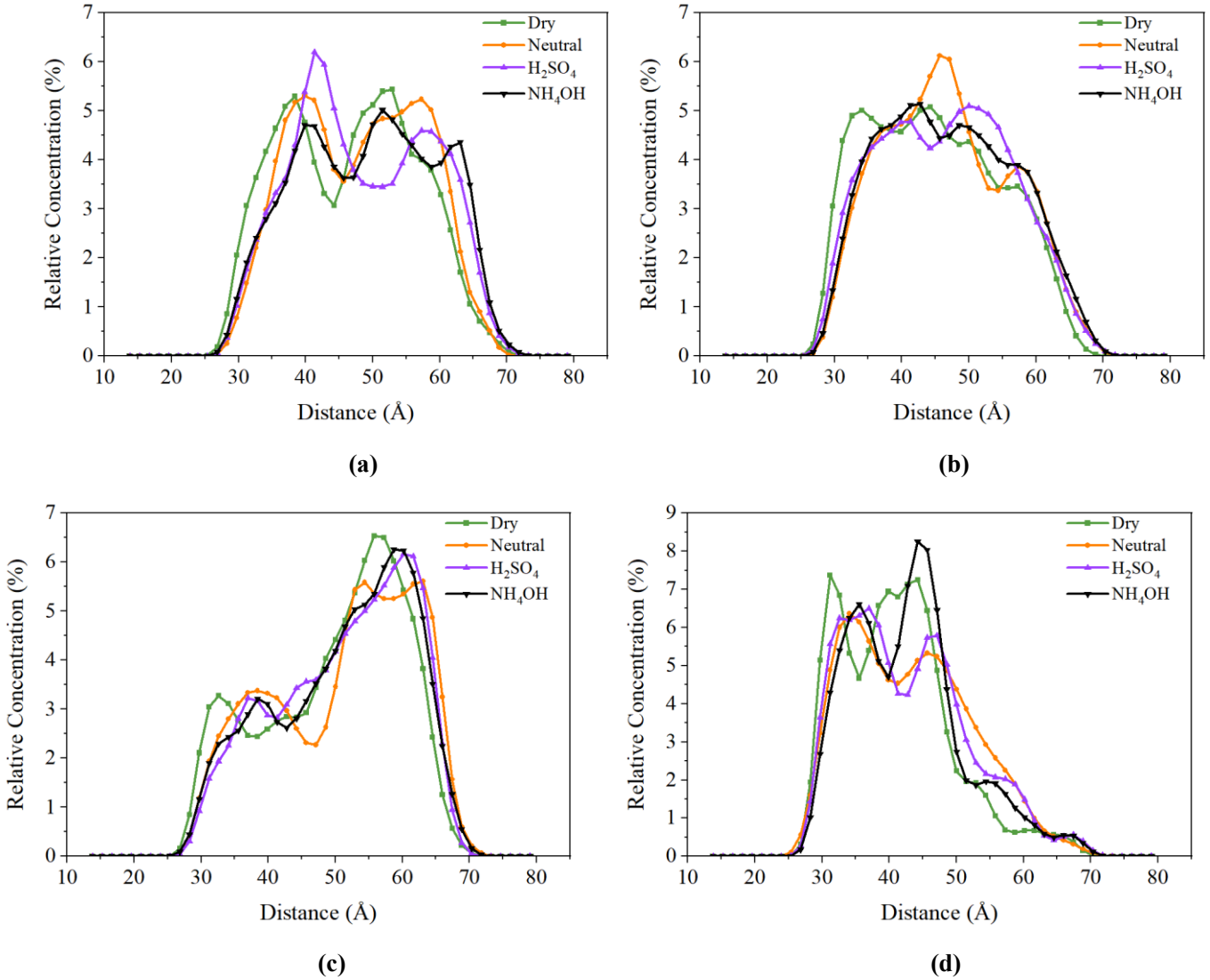

Fig. 14. Relative concentration distribution of SARA fractions in quartz-asphalt system under different environments along z direction: (a) Asphaltene, (b) Resin, (c) Aromatic, and (d) Saturate.

3.4 Effect of acidity and alkalinity of aqueous solution on molecular transition mobility of asphalt on aggregate surface

The mean square displacement (MSD) curves of the SARA components of asphalt binder on the surface of calcite and quartz are shown in Fig. 15 and Fig. 16, respectively. It can be seen from the MSD curves of the calcite system that the slope of each component of asphalt is roughly the same in the dry and acidic and alkaline water environments. However, it is significantly smaller than that in the neutral water condition. This may be due to the fact that the neutral water molecular layer is not charged and the distance between the calcite and asphalt is increased, resulting in a weakened electrostatic interaction between the aggregate and the polar components of asphalt and an enhanced migration ability of polar molecules. On the surface of quartz, the migration rate of the four components of asphalt in the dry environment is basically lower than that in the remaining three wet environments, and the migration rate of resin and aromatic fractions is significantly different from the other water environments. The possible reason is that the presence of water molecules at the asphalt-quartz interface increases the distance between asphalt molecules and aggregate, resulting in a decrease in van der Waals force at the interface of these two materials. Therefore, the asphalt components have a stronger migration capacity.

Each MSD curve shown in Fig. 15 and Fig. 16 is linearly fitted, and the diffusion coefficients of asphalt components under different environmental conditions can be calculated from the slope of the fitted curves and equation (10). The calculation results are summarized in Table 3. In the calcite system and quartz system, the slopes of light components such as aromatic and saturate fractions in the asphalt layer under the three wet environments are greater than those under the dry environment. This indicates that when water is present at the interface, the interaction of the light components in asphalt is reduced, which are more likely to migrate. Therefore, when there are water molecules at the aggregate-asphalt interface, it will cause the rearrangement of asphalt components and change the asphalt structure, further leading to the macro-scale adhesive failure of the asphalt-aggregate system.

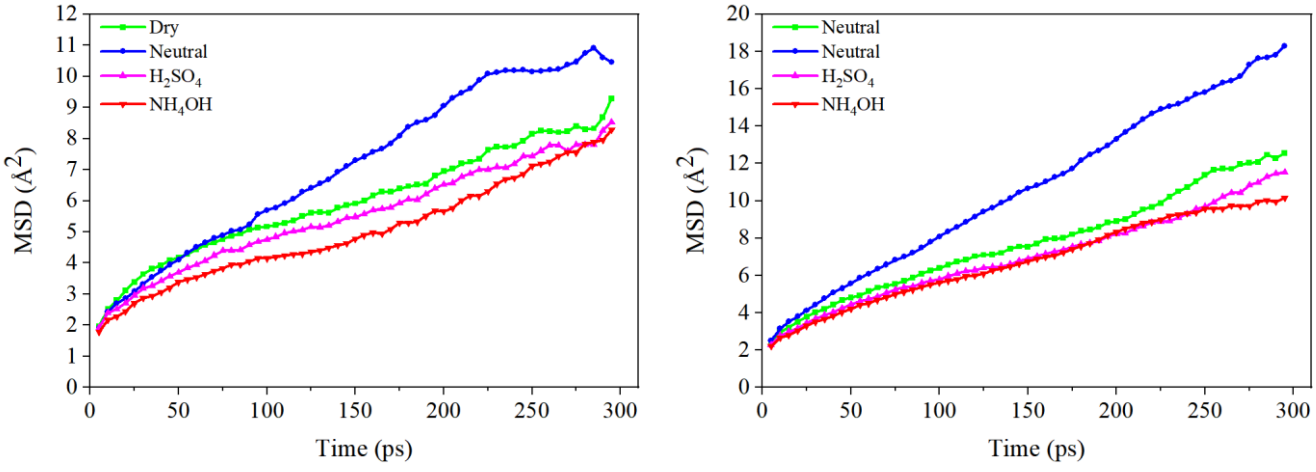

(a) (b)

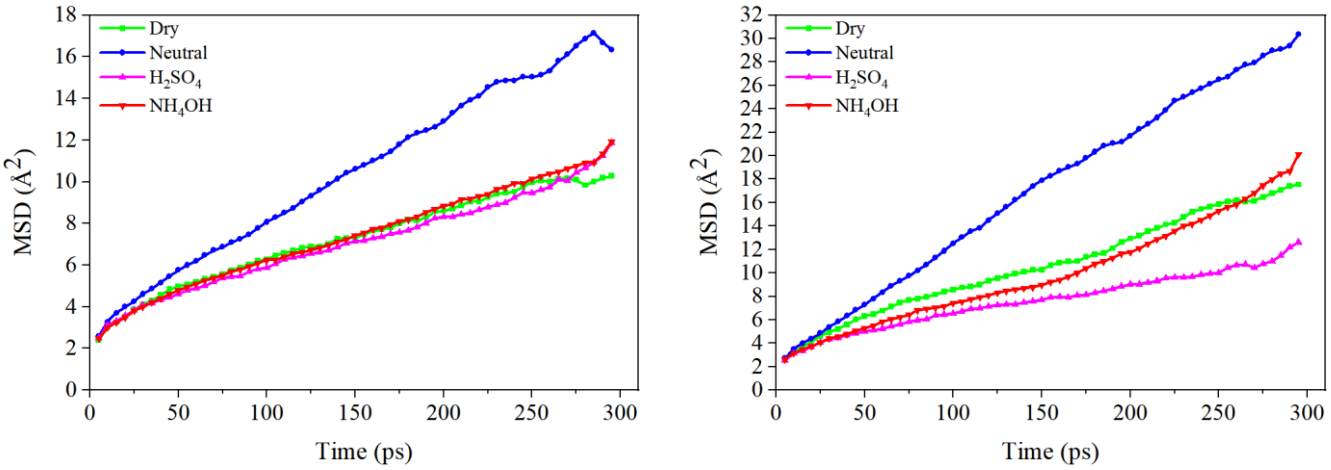

Fig. 15. MSD of SARA fractions of asphalt in different environments in calcite-asphalt system for (a), (b) Resin, (c) Aromatic, and (d) Saturate.

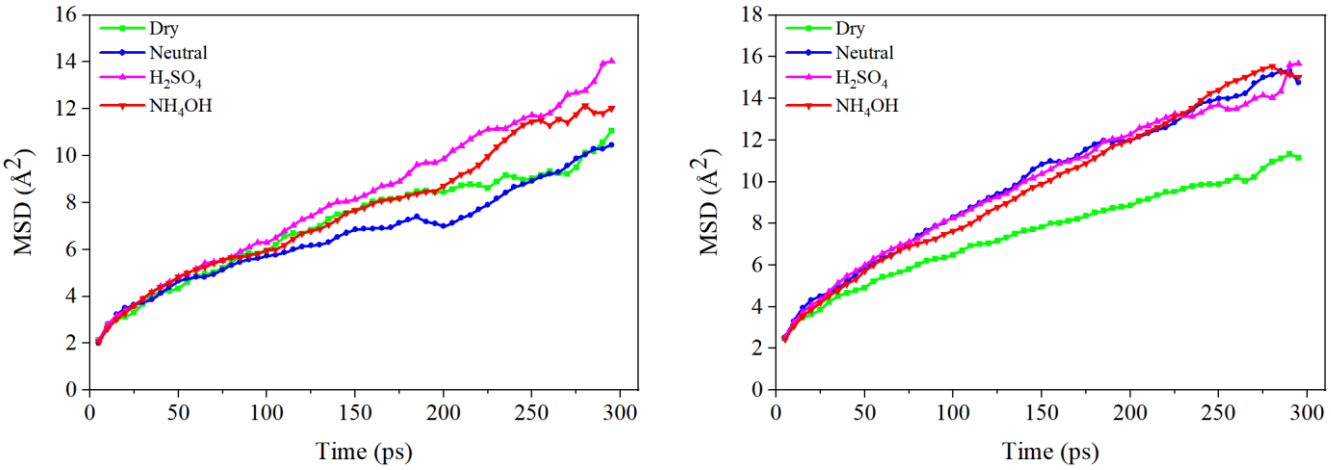

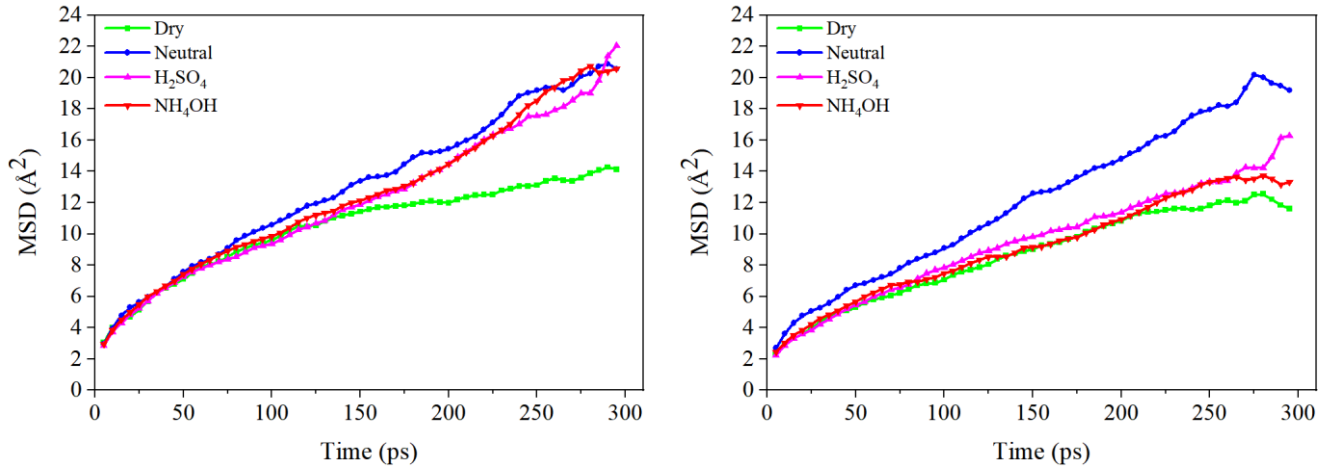

Fig. 16. MSD of SARA fractions of asphalt in different environments in quartz-asphalt system for (a) Asphaltene, (b) Resin, (c) Aromatic, and (d) Saturate.

Table 3 Diffusion coefficients of SARA fractions under different environments

Aggregate	SARA Component	Dry	Neutral	H_2SO_4	NH_4OH
Calcite	Asphaltene	0.003	0.005	0.003	0.003
	Resin	0.005	0.009	0.005	0.004
	Aromatic	0.004	0.008	0.004	0.005
	Saturate	0.009	0.016	0.005	0.009
Quartz	Asphaltene	0.004	0.004	0.006	0.005
	Resin	0.004	0.007	0.007	0.007
	Aromatic	0.005	0.010	0.009	0.009
	Saturate	0.006	0.010	0.007	0.006

3.5 Effect of acidity and alkalinity of aqueous solution on adhesion energy of asphalt-aggregate system

The calculation results of the adhesion work for calcite-asphalt and quartz-asphalt in dry, neutral water, ammonia, sulfuric acid solution environments are presented in Fig. 17. From the adhesion work results, it can be seen that the interaction between calcite and asphalt is mainly electrostatic interaction, while that between quartz and asphalt is mainly van der Waals interaction. This is because calcite is an ionic compound with a large number of positive and negative charges, while quartz is a covalent compound. At the same time, the adhesion work value in the dry system is in the range of 110-150mJ/m^2, and the adhesion work value in the wet systems is in the range of 40mJ/m^2~80mJ/m^2, which are consistent with those reported in previous studies [45]-[47]. The calculation results of the adhesion work show that when there are water molecules at the aggregate-asphalt interface, the adhesion between asphalt and aggregate will decrease significantly. In the calcite simulation systems, the work of adhesion between aggregate and asphalt can be sorted as follows: dry environment > neutral water environment > sulfuric acid solution environment > ammonia aqueous solution environment. Compared with the dry environment, the adhesion energy between aggregate and asphalt is reduced by 45.3%, 46.8% and 48.8% in the environments of neutral water, sulfuric acid solution and ammonia aqueous solution, respectively. However, in the quartz simulation systems, the adhesion of aggregate-asphalt can be sorted in the following order: dry environment > sulfuric acid solution environment > neutral water environment > ammonia aqueous solution environment. Compared with the dry condition, the work of adhesion between aggregate and asphalt is decreased by 53.2%, 48.4% and 58.4% in the environment of neutral water, sulfuric acid solution and ammonia aqueous solution, respectively. It should be noted that when the quartz is selected as the aggregate, the adhesion of asphalt-aggregate system decreases more when it is subjected to the wet conditions.

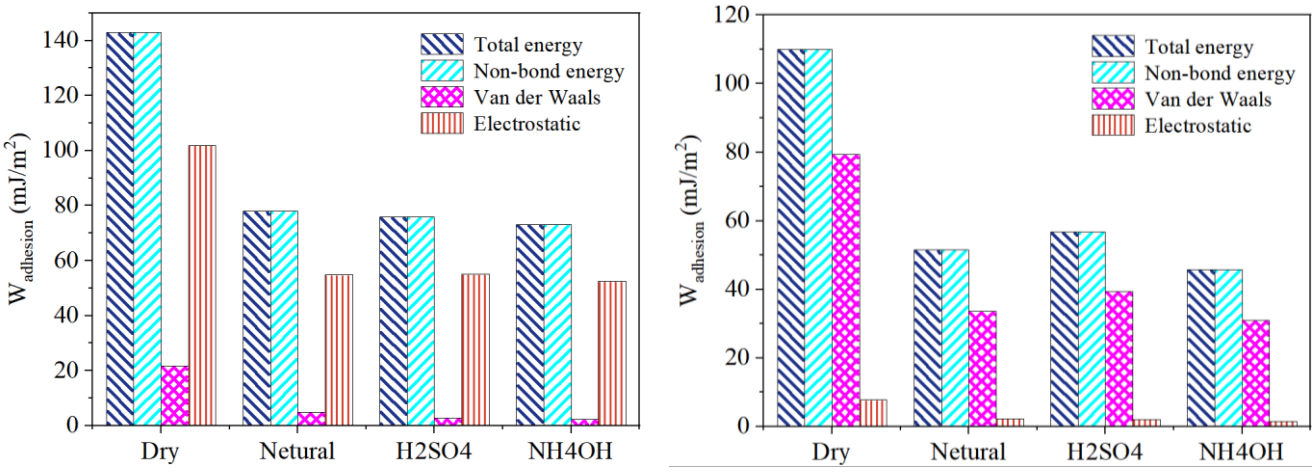

Fig. 17. Work of adhesion between aggregate-asphalt in different environments for (a) calcite-asphalt system, and (b) silica-asphalt system.

The calculation results of the adhesion work between the asphalt component and aggregate are shown in Fig. 18. It is clear that in the calcite and quartz systems, resin is the asphalt component that contributes the most to the adhesion of the overall asphalt-aggregate system, followed by aromatic. In the four environments, the adhesion work between these two asphalt components and aggregate accounts for more than 65% of the total adhesion work of asphalt-aggregate system. Although the polarity of asphaltene component in asphalt is stronger than that of resin and aromatic, the content of this component is relatively low in asphalt binder. Besides, it is worthy to mention that the saturate is intrinsically a non-polar component. Therefore, asphaltene and saturate components contribute less to the adhesion between aggregate and asphalt in comparison with the other two asphalt components. Also, it should be noted that the distance of each component of asphalt to the surface of the aggregate has an important influence on its adhesion performance with the aggregate, and a larger distance normally results in a lower adhesion. According to the adhesion work between the aggregate and the asphalt component derived from the Materials Studio software, it was possible to roughly rank the distance between each component and the surface of the aggregate. The estimates are found to be in good agreement with those presented in section 3.3, which validates the reliability of the simulation models.

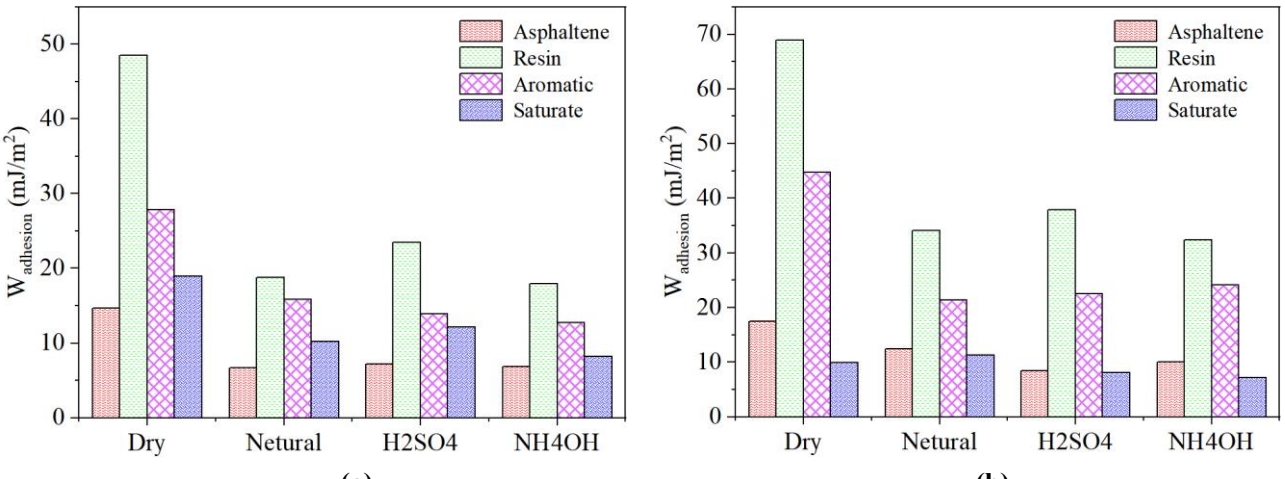

Fig. 18. Componential adhesion work of (a) calcite-asphalt system, and (b) silica-asphalt system.

3.6 Effect of acidity and alkalinity of aqueous solution on water stability of asphalt-aggregate system

Fig. 19 shows the calculation results of ER value for the asphalt-aggregate systems under different water environments. As mentioned earlier, the larger the ER value of the asphalt-aggregate system, the higher the water stability. Apparently, the acidity and alkalinity of water environment have different impacts on the water stability of asphalt-aggregate system for different types of aggregate used. When taking the calcite as the aggregate, the water stability of asphalt-aggregate in terms of water environment can be ranked as follows: neutral water environment > acidic water environment > alkaline water environment. However, when the quartz is used as the aggregate, this ranking is changed to: acidic water environment > neutral water environment > alkaline water environment. These two rankings are consistent with the analysis on the molecular structure and interaction energy of the asphalt-aggregate systems presented in Section 3.1 and Section 3.2.

It is worth mentioning that the adhesion work and ER value in wet environments reflect different aspects of water stability in asphalt-aggregate system. Indicatively, the adhesion work under the wet environment reflects the residual adhesion between aggregate and asphalt when water molecules arrive at the asphalt-aggregate interface. In this sense, a higher value of adhesion work between aggregate-asphalt indicates that the adhesion between aggregate and asphalt is better when the same number of water molecules intrude on the interface of aggregate and asphalt. The ER value, on the other hand, represents the ability of the asphalt-aggregate system to resist the water erosion. As can be seen from Equation (13), the ER value is inversely proportional to the absolute value of the debonding work. Considering that the debonding work is intrinsically negative because the affinity of aggregate to water is stronger than that to asphalt, the erosion of water molecules to the asphalt-aggregate interface is a thermodynamic spontaneous process and no external work is required [14]. Thus, a smaller ER value signifies that more water molecules are likely to invade the aggregate-asphalt interface. Therefore, for the sake of accurately evaluating the water stability of asphalt-aggregate system, it is necessary to consider the adhesion energy and the ER simultaneously.

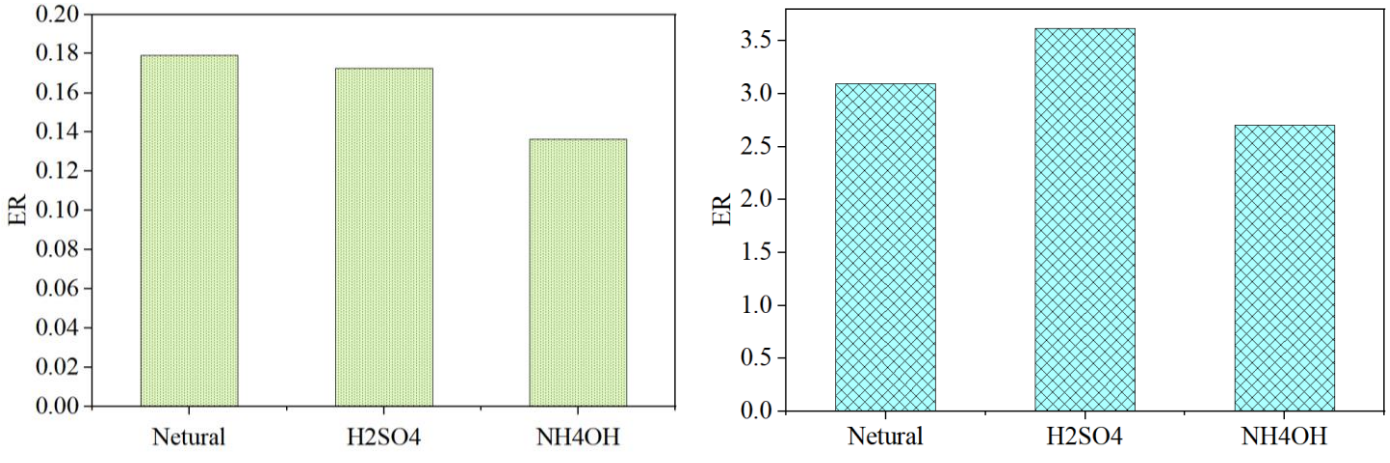

Fig. 19. Calculated energy ratio values of (a) calcite-asphalt system, and (b) silica-asphalt system.

4. Conclusions and on-going work

In this study, the influence of acidity and alkalinity of the water environment on the water stability of asphalt-aggregate system were investigated through the Molecular Dynamics (MD) simulation. The asphalt-aggregate interface models in dry, neutral water, acidic and alkaline water environments were first established. The structural changes of the asphalt-aggregate interface and the distribution of the four components (SARA) of asphalt under three different wet environments were then analyzed. The potential energy parameters were extracted from the MD software and subsequently used to calculate the adhesion work between the aggregate and asphalt as well as the aggregate and asphalt component under different environments. The ER value was finally determined to quantify the water stability of asphalt-aggregate system. The main conclusions of this study are as follows:

(1) The acidity and alkalinity of the water environment will affect the structure of asphalt and the distribution of asphalt components. In acidic and neutral water environments, asphalt molecules are grid-shaped. However, in alkaline water environments, asphalt molecules are distributed in a columnar pattern independent and parallel to each other.

(2) In different acidic and alkaline water environments, the interface of the same aggregate-asphalt systems has similar nanostructure. However, distinct differences in the interfacial nanostructure can be observed for different aggregate systems. This is mainly ascribed to the different interaction mechanisms between asphalt and aggregate molecules in different aggregate systems. In the calcite system, the interaction between the aggregate-water-asphalt is mainly driven by electrostatic force, which is however driven by the van der Waals force in the quartz system.

(3) When there are water molecules existing at the asphalt-aggregate interface, the distance between the aggregate and asphalt will be increased and the asphalt will be detached from the aggregate surface. In such a detachment process, the four components (SARA) of asphalt have different interaction mechanisms with the water molecules and aggregate in the presence of neutral, acidic, and alkaline aqueous solutions. Therefore, different asphalt component molecules migrate at different diffusion rates, which results in the redistribution of asphalt components and the change of colloid structure of asphalt, further causing the macroscopic adhesive failure of asphalt-aggregate system.

(4) The water stability of the calcite-asphalt system in acidic and alkaline environments is worse than that in neutral water environment, which can be ascribed to the higher activity of the ammonia and sulfuric acid solutions as compared to that of the neutral water. When invading the asphalt-calcite interface, the ammonia and sulfuric acid solution molecules are in closer contact with aggregate and asphalt, making the asphalt more easily to strip from the aggregate. However, for quartz-asphalt system, the water stability in neutral water environment is worse than that in acidic water environment, but better than that in alkaline water environment. The possible reason is that the sulfuric acid solution

at the asphalt-quartz interface may have a significant aggregation effect, which will increase the contact area between aggregate and asphalt.

(5) To accurately quantify the water stability of asphalt-aggregate system, it is necessary to consider the adhesion energy and the energy ration (ER) value simultaneously. This is because the former reflects the residual adhesion between aggregate and asphalt when water molecules arrive at the asphalt-aggregate interface, while the latter is associated with the ability of the asphalt-aggregate system to resist the water erosion.

As a preliminary study, this piece of work focuses on unveiling the influence mechanism of acidity and alkalinity of water environment on the water stability of asphalt-aggregate system from a nano-scale perspective. The rankings of the water ability of the asphalt-aggregate obtained in this study for the different water environments will be further verified through the water damage performance test, such as the freeze-thaw splitting test and the net adsorption test. More importantly, in addition to the nano-scale investigation, the micro- and macro-scale investigations will be conducted on the asphalt-aggregate system under various water environments in the future to provide an in-depth understanding of the water damage of asphalt pavement resulted from the alteration of water pH.

Acknowledgments

The authors acknowledge the financial support of the National Natural Science Foundation of China (Grant Number: 52108407 & 52108410) and the Fundamental Research Funds for the Central Universities (Grant Number: 2020kfyXJJS123).

Conflict of Interest

The authors declare that they have no conflict of interest.

References

[1]Liu X., Li B., & Jia M. Effect of short-term aging on interface-cracking behaviors of warm mix asphalt under dry and wet conditions. Constr. Build. Mater. 261 (2020) 119885. DOI: 10.1016/j.conbuildmat.2020.119885.

[2]Caro S., Masad E., Bhasin A., & Little D. N. Moisture susceptibility of asphalt mixtures, Part 1: mechanisms, Int. J. Pavement Eng. 9 (2008) 81–98. DOI: 10.1080/10298430701792128.

[3]Chen X., & Huang B, Evaluation of moisture damage in hot mix asphalt using simple performance and superpave indirect tensile tests, Constr. Build. Mater. 22 (2008) 1950–1962. DOI: 10.1016/j.conbuildmat.2007.07.014.

[4]Xu T., Wang H., Li Z., & Zhao Y. Evaluation of permanent deformation of asphalt mixtures using different laboratory performance tests, Constr. Build. Mater. 53 (2014) 561–567. DOI: 10.1016/j.conbuildmat.2013.12.015.

[5]Dong M., Gao Y., Li L., et al. Viscoelastic micromechanical model for dynamic modulus prediction of asphalt concrete with interface effects, J. Central South Univ. 23 (2016) 926–933. DOI: 10.1007/s11771-016-3140-y.

[6]Moraes R., Velasquez R., & Bahia H. Measuring the effect of moisture on asphalt-aggregate bond with the asphalt bond strength test. Transportation Research Record, 2209 (2011) 70–81. DOI: 10.3141/2209-09.

[7]Zhang J., Gordon D. A., James G., & Alex K. A. Moisture damage evaluation of aggregate–asphalt bonds with the respect of moisture absorption, tensile strength and failure surface, Road Materials and Pavement Design, 18:4 (2017) 833-848. DOI: 10.1080/14680629.2017.1286441.

[8]Liu Z., Cao L., Zhou T., et al. Multiscale Investigation of Moisture-Induced Structural Evolution in Asphalt-Aggregate Interfaces and Analysis of the Relevant Chemical Relationship Using Atomic Force Microscopy and Molecular Dynamics. Energy & Fuels. 34(4) (2020) 4006-4016. DOI: 10.1021/acs.energyfuels.9b03270.

[9]Xu G., Yu Y., Cai D., et al. Multi-scale damage characterization of asphalt mixture subject to freeze-thaw cycles. Constr. Build. Mater. 240 (2020) DOI: 10.1016/j.conbuildmat.2019.117947.

[10]Wang H., et al. Molecular dynamics simulation of asphalt-aggregate interface adhesion strength with moisture effect. Int. J. Pavement Eng. 18(5) (2017) 414-423. DOI: 10.1016/j.conbuildmat.2019.117947.

[11]Cui W., Huang W., Hu B., et al. Investigation of the Effects of Adsorbed Water on Adhesion Energy and Nanostructure of Asphalt and Aggregate Surfaces Based on Molecular Dynamics Simulation. Polymers. 12(10) (2020) DOI: 10.3390/polym12102339.

[12]Cui W., et al. The Effect of Moisture on the Adhesion Energy and Nanostructure of Asphalt-Aggregate Interface System Using Molecular Dynamics Simulation. Molecules. 25(18) (2020). DOI: 10.3390/molecules25184165.

[13]Gao Y., et al. Impact of minerals and water on asphalt-mineral adhesion and debonding behaviours using molecular dynamics simulations. Construction and Building Materials. 171 (2018) 214-222. DOI: 10.1016/j.conbuildmat.2018.03.136.

[14]Sun W. and Wang H. Moisture effect on nanostructure and adhesion energy of asphalt on aggregate surface: A molecular dynamics study. Applied Surface Science 510 (2020) DOI: 10.1016/j.apsusc.2020.145435.

[15]Arabani, M., et al. Evaluation of the Effect of Dust and Soot on Runoff Acidity and Moisture Sensitivity of Asphalt Mixtures Using Thermodynamic and Mechanical Methods. Journal of Materials in Civil Engineering 32(11) (2020). DOI: 10.1061/(ASCE)MT.1943-5533.0003397.

[16]Xie S, Wang S, Yu Y, et al. Study on the change trend of acid rain in China from 2003 to 2018. China's environmental monitoring. 4(4) (2020) 80-88.

[17]Yoon H., & Tarrer A. Effect of Aggregate Properties on Stripping. Transportation Research Record, 1171 (1989) 37-43.

[18]Hu C., Zhou Z., Chen G. Effects of different types of acid rain on water stability of asphalt pavement. Construction and Building Materials, 322 (2022) 126308. DOI: 10.1016/j.conbuildmat.2022.126308.

[19]Hughes R., Lamb D., & Pordes O. Adhesion in asphalt macadam. Journal of Applied Chemistry, 10 (1960) 433-444.

[20]Li D., & Greenfield M. Chemical compositions of improved model asphalt systems for molecular simulations, Fuel 115 (2014) 347–356. DOI: 10.1016/j.fuel.2013.07.012.

[21]Xu G. & Wang H. Molecular dynamics study of interfacial mechanical behavior between asphalt binder and mineral aggregate. Construction and Building Materials 121 (2016) 246-254. DOI: 10.1016/j.conbuildmat.2016.05.167.

[22]Long Z., et al. Analysis of interfacial adhesion properties of nano-silica modified asphalt mixtures using molecular dynamics simulation. Construction and Building Materials 255 (2020). DOI: 10.1016/j.conbuildmat.2020.119354.

[23]Ma X., et al. Molecular dynamics simulation of the asphalt-aggregate system and the effect of simulation details. Construction and Building Materials 285 (2021). DOI: 10.1016/j.conbuildmat.2021.122886.

[24]Gao M., et al. Molecular dynamics investigation of interfacial adhesion between oxidised asphalt and mineral surfaces. Applied Surface Science 479 (2019) 449-462. DOI: 10.1016/j.apsusc.2019.02.121.

[25]Khan A., Redelius P., & Kringos N. Evaluation of adhesive properties of mineral-bitumen interfaces in cold asphalt mixtures, Constr. Build. Mater.125 (2016) 1005–1021. DOI: 10.1016/j.conbuildmat.2016.08.155.
[26]Read J. D. Whiteoak, The shell asphalt handbook, Thomas Telfold, London, 2003.
[27]Khabaz F. & Khare R. Glass Transition and Molecular Mobility in Styrene-Butadiene Rubber Modified Asphalt. Journal of Physical Chemistry B 119(44) (2015) 14261-14269. DOI: 10.1021/acs.jpcb.5b06191.
[28]Chu L., et al. Effects of aggregate mineral surface anisotropy on asphalt-aggregate interfacial bonding using molecular dynamics (MD) simulation. Construction and Building Materials 225 (2019) 1-12. DOI: 10.1016/j.conbuildmat.2019.07.178.
[29]Sun H. COMPASS: An ab initio force-field optimized for condensed-phase applications - Overview with details on alkane and benzene compounds. Journal of Physical Chemistry B, 102(38) (1998) 7338-7364. DOI: 10.1021/jp980939v.
[30]Sun H., et al. COMPASS II: extended coverage for polymer and drug-like molecule databases. Journal of Molecular Modeling, 22(2) (2016). DOI: 10.1007/s00894-016-2909-0.
[31]Xu G. & Wang H. Study of cohesion and adhesion properties of asphalt concrete with molecular dynamics simulation. Computational Materials Science, 112 (2016) 161-169. DOI: 10.1016/j.commatsci.2015.10.024.
[32]Huang M., et al. Study of diffusion characteristics of asphalt-aggregate interface with molecular dynamics simulation. International Journal of Pavement Engineering, 22(3) (2021) 319-330. DOI: 10.1080/10298436.2019.1608991.
[33]Du Z. & Zhu X. Molecular Dynamics Simulation to Investigate the Adhesion and Diffusion of Asphalt Binder on Aggregate Surfaces. Transportation Research Record, 2673(4) (2019) 500-512. DOI: 10.1177/0361198119837223.
[34]Dong Z., Liu Z., Wang P., Gong X. Nanostructure characterization of asphalt-aggregate interface through molecular dynamics simulation and atomic force microscopy. Fuel, 189 (2017) 155–163. DOI: 10.1016/j.fuel.2016.10.077.
[35]Xu M., et al. Diffusion characteristics of asphalt rejuvenators based on molecular dynamics simulation. International Journal of Pavement Engineering, 20(5) (2019) 615-627. DOI: 10.1080/10298436.2017.1321412.
[36]Li C., et al. Method for Evaluating Compatibility between SBS Modifier and Asphalt Matrix Using Molecular Dynamics Models. Journal of Materials in Civil Engineering, 33(8) (2021). DOI： 10.1061/(ASCE)MT.1943-5533.0003863.
[37]Long Z, et al. Influence of sea salt on the interfacial adhesion of asphalt-aggregate systems by molecular

748 dynamics simulation. Construction and Building Materials, 336 (2022). DOI:
749 10.1016/j.conbuildmat.2022.127471.
750 [38]Luo L., et al. Molecular dynamics analysis of moisture effect on asphalt-aggregate adhesion considering
751 anisotropic mineral surfaces. Applied Surface Science, 527 (2020). DOI: 10.1016/j.apsusc.2020.146830.
752 [39]Bhasin A., et al. Surface free energy to identify moisture sensitivity of materials for asphalt mixes.
753 Transportation Research Record 2001 (2007) 37-45. DOI: 10.3141/2001-05.
754 [40]Zhang H., et al. Molecular dynamics study on improvement effect of bis (2-hydroxyethyl) terephthalate
755 on adhesive properties of asphalt-aggregate interface. Fuel, 285 (2021). DOI: 10.1016/j.fuel.2020.119175.
756 [41]Yu T., et al. Microscopically analyzed the interface behavior characteristics of acid precipitation on asphalt
757 surface. Water Science and Technology, 84(8) (2021) 2068-2078. DOI: 10.2166/wst.2021.412.
758 [42]Wei J., Dong F., Li Y., et al. Relationship analysis between surface free energy and chemical composition
759 of asphalt binder. Construction and Building Materials, 71 (2014) 116-123. DOI:
760 10.1016/j.conbuildmat.2014.08.024.
761 [43]Guo F., Zhang J., Pei J., et al. Study on the Mechanical Properties of Rubber Asphalt by Molecular
762 Dynamics Simulation. Journal of Molecular Modeling, 25(12) (2019). DOI: 10.1007/s00894-019-4250-x.
763 [44]Li L., Guo M., & Zeng C. Influence of the Chemical Composition of Asphalt and the 3D Morphology of
764 the Aggregate on Contact Surface Adhesion. Advances in Civil Engineering, (2021) 8870295. DOI:
765 10.1155/2021/8870295.
766 [45]Ji J., Yao H., Liu L., et al. Adhesion Evaluation of Asphalt-Aggregate Interface Using Surface Free Energy
767 Method. Applied Sciences-Basel, 7(2) (2017). DOI: 10.3390/app7020156.
768 [46]Tan Y., & Guo M. Using surface free energy method to study the cohesion and adhesion of asphalt mastic.
769 Construction and Building Materials, 47 (2013) 254-260. DOI: 10.1016/j.conbuildmat.2013.05.067.
770 [47]Hamedi G. M., Asadi M., Nejad F. M., & Esmaeeli M. R. Applying asphalt binder modifier in reducing
771 moisture-induced damage of asphalt mixtures. European Journal of Environmental and Civil Engineering.
772 (2019) 2039-2056. DOI: 10.1080/19648189.2019.1615554.

Appendix:

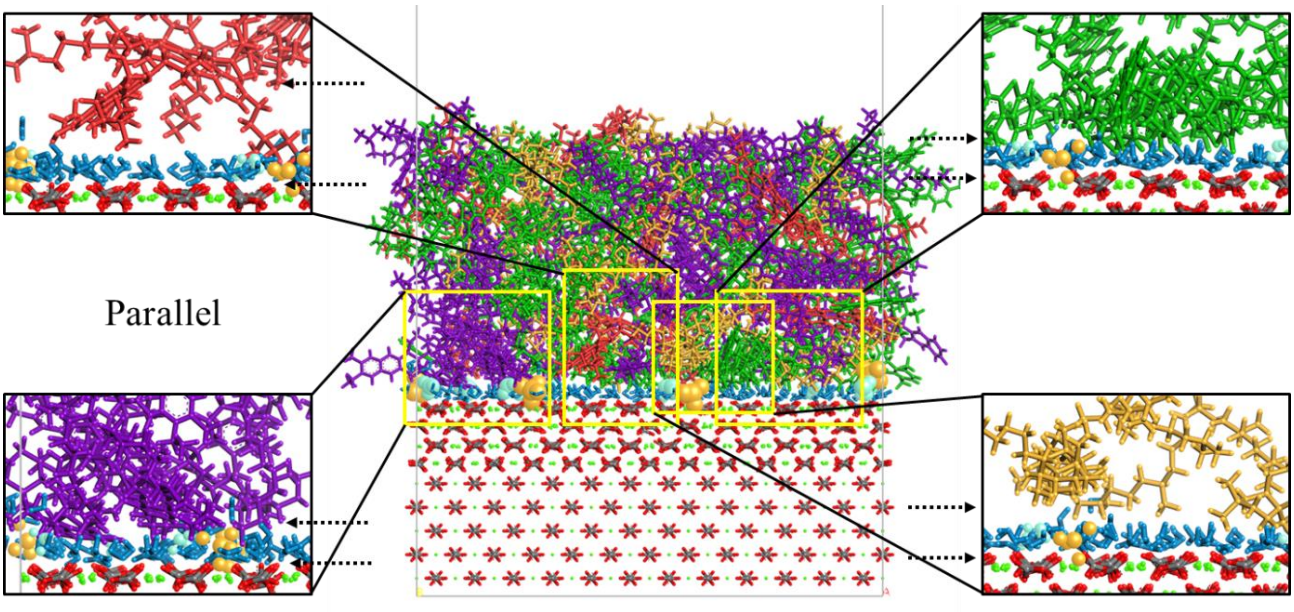

Appendix Fig.1. Molecular interaction of asphalt-H_2SO_4-calcite

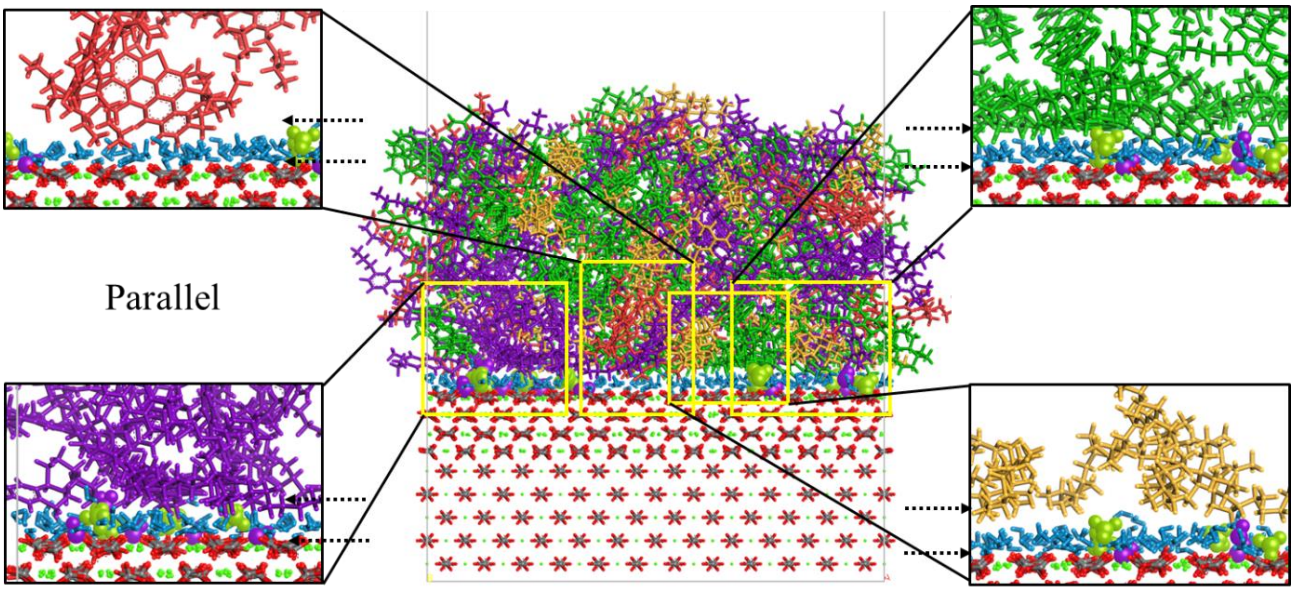

Appendix Fig.2. Molecular interaction of asphalt-NH_4OH-calcite

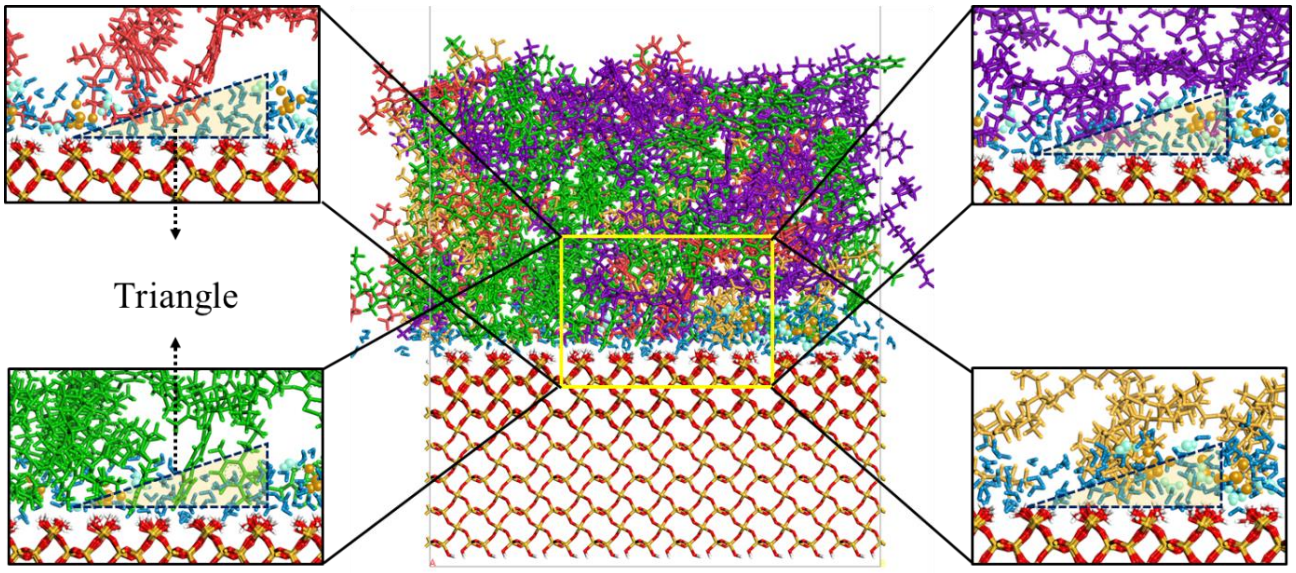

Appendix Fig.3. Molecular interaction of asphalt-H_2SO_4-quartz

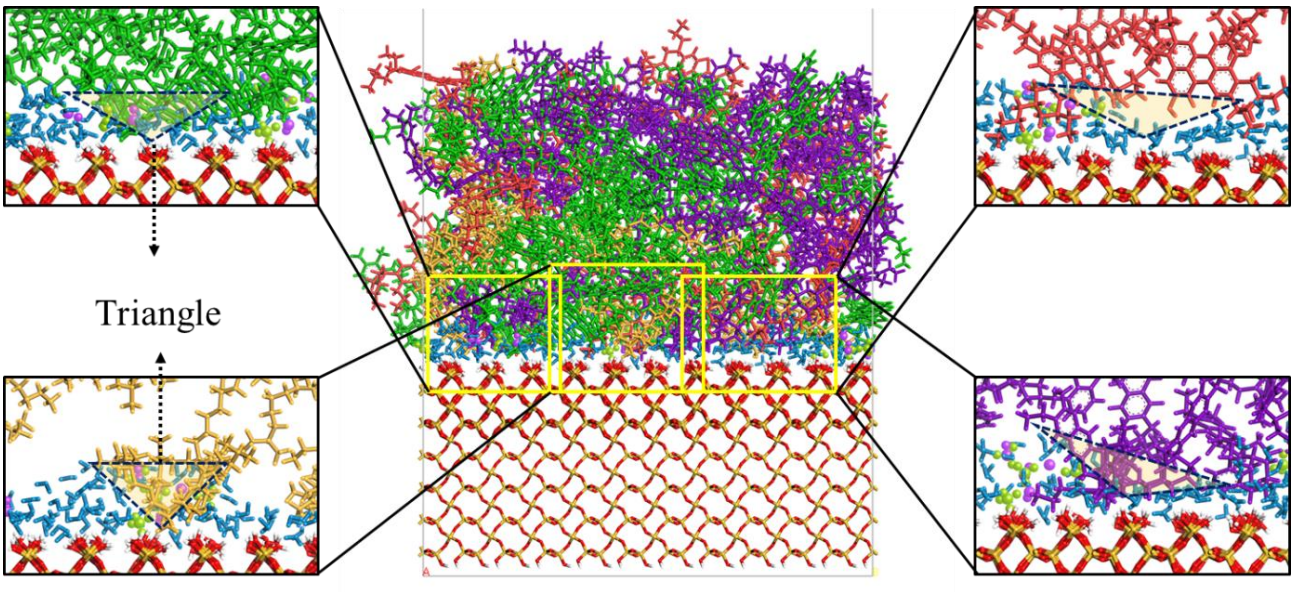

Appendix Fig.4. Molecular interaction of asphalt-NH_4OH-quartz